

AN AUTONOMOUS DIGGING VEHICLE

Except where reference is made to the work of others, the work described in this thesis is my own or was done in collaboration with my advisory committee. This thesis does not include proprietary or classified information.

Courtney A. Guasti

Certificate of Approval:

Jeffrey W. Fergus
Associate Professor
Materials Engineering

William F. Gale, Chair
Professor
Materials Engineering

Ruel A Overfelt
Professor
Materials Engineering

Stephen L. McFarland
Dean
Graduate School

AN AUTONOMOUS DIGGING VEHICLE

Courtney Allen Guasti

A Thesis

Submitted to

the Graduate Faculty of

Auburn University

in Partial Fulfillment of the

Requirements for the

Degree of

Master of Science

Auburn, Alabama
August 7, 2006

AN AUTONOMOUS DIGGING VEHICLE

Courtney Allen Guasti

Permission is granted to Auburn University to make copies of this thesis at its discretion, upon the request of individuals or institutions and at their expense. The author reserves all publication rights.

Signature of Author

Date of Graduation

VITA

Courtney Guasti, son of Victoria Rhodes and John Aruzza, was born on March 7, 1979, in Burlington, Vermont. He graduated Brooks High School in Killen, Alabama with an “Advanced Academic Diploma” in May of 1997. He then attended Auburn University on scholarship where he obtained a Bachelors of Science in Textile Engineering in May 2001. After working for a year he then returned in August of 2002 to enter the Graduate School at Auburn University. He married Abigail Gray, daughter of Don and Mona Gray of Killen, Alabama on July 16, 2005. After finishing his coursework, Courtney was employed by the U.S. Army Aviation & Missile Research, Design and Engineering Center, located on the Redstone Arsenal in Huntsville, Alabama.

THESIS ABSTRACT

AN AUTONOMOUS DIGGING VEHICLE

Courtney Allen Guasti

Master of Science, August 7, 2006
(B.S. Textile Engineering, Auburn University, 2001)

127 Typed Pages

Directed by Dr. William Gale

This project is intended to develop a self-guided digging vehicle for various applications. Hence, the main focus for this vehicle is to have the ability to dig through loose soils. This project has focused on key digging technologies such as the use of shape memory alloys (SMAs) to motor power, precision motors to power conical and helical augers and biological movements as observed in “fossorial” creatures.

Initially SMAs were selected as the source of motion to drive an auger to move the vehicle through the soil; whereas precision motors have become more promising for this purpose and became the second phase of this project. It was observed that SMAs of a feasible geometry could not produce the torque required to move the vehicle. Small SMAs have a low energy conversion efficiency (less than 5%) and cannot handle large loads. Large SMAs can handle larger loads, however these seem to experience shape “amnesia” at an increased rate (with currents over 10 A), when compared with standard SMAs.

The use of an electric motor offers long lasting capabilities and when used with currents of around 15 A can produce the torque needed to bury itself sufficiently with customized augers.

The third phase of this project looks at researching digging creatures and their movements to move through the earth. To scale down the amount of creatures involved in the research, an initial criterion of being “fossorial” was established. Upon selection of the creatures to be researched, specific questions were created to maximize the time researching each creature and not researching useless information. A weighting system was established ranking the following criteria deemed important for a digging vehicle: speed, power, depth, material substance, mechanical complexity, geographic range and size of organism. This ranking consisted of a scale of 1-5, with a score of one being harmful and a score of 5 being important. Three scenarios were then created, giving each of the seven metrics different percentages based on the importance of each: Scenario 1, small body (≤ 30 cm; 12 in) at low depths (≤ 152 cm; 60 in); scenario 2, small body (≤ 30 cm; 12 in) at medium depths (152 cm; 60 in – 610 cm; 240 in) and scenario 3, medium body (30 cm; 12 in – 91 cm; 36 in) at deep depths (≥ 610 cm; 240 in). Each creature was then given a final score and compared to each other, with the highest score from each scenario receiving the chance to be selected for further modeling.

Although more information is needed for all the creatures to identify an animal most worthy of modeling, the available information indicates that the Townsend mole is the creature worthy of being selected.

ACKNOWLEDGMENTS

I would like to thank Dr. William Gale for his support and guidance throughout my graduate career. The professional traits that Dr. Gale has taught me will be invaluable throughout my career. Thank you Dave Lindahl for his patience and guidance throughout the many difficulties faced during my projects. Thank you to Dr. Jeffery Fergus and Dr. Ruel Overfelt for their help, advice and guidance given. I would also like to thank Ben Beyer, Robert Love and Chris Long for their relentless effort in helping during all aspects of the research.

I especially want to thank my wife for sticking with me during my graduate career, even though she thought I would never finish. Without your help, I wouldn't be where I am today. I love you!

Last but not least, I would like to thank all my friends who have made my years at Auburn enjoyable and very memorable. May we all meet up in the years to come.

Style manual or journal used: Journal of Metallurgical Transactions A.

Computer software used: Microsoft Word 2000, Microsoft Excel 2000

TABLE OF CONTENTS

LIST OF TABLES	xiv
LIST OF FIGURES	xv
1. INTRODUCTION	1
2. LITERATURE REVIEW	4
2.1 History of Drilling	4
2.2 Earthmoving Equipment.....	5
2.3. Augers	8
2.4. Revolutionary Drilling.....	10
2.5. Shape Memory Alloys.....	10
2.6. Mechanical Biomimetic Devices.....	13
2.7. Wildlife Research	16
2.8. Autonomous Technology	20
2.8.1 Power Supply.....	20
2.8.2 Single Vehicle vs Group Approach.....	22
2.8.3 Communication	23
3. RESEARCH OBJECTIVES	25
4. MATERIALS AND METHODS.....	27
4.1 SMA Testing	27
4.2 Auger Testing.....	33
4.2.1 Electrical Motor.....	30

4.2.2	Conical Augers	30
4.2.3	Helical Augers	33
4.2.4	Torque Requirements	35
4.2.5	Push Test	36
4.2.6	Pull Test.....	38
4.2.7	Colored Sand Experiment.....	39
4.2.8	Customized Auger	41
	4.2.8.1 Plain Sand Experiments.....	42
	4.2.8.2 Sand Mixture Experiments.....	43
	4.2.8.3 Compacted Sand Mixture Experiments.....	44
	4.2.8.4 Torque Requirements of Customized Auger.....	45
4.2.9	Digging Energy Requirements	45
4.3	Vehicle Experiments	45
	4.3.1 Earthworm Concept.....	45
	4.3.2 Friction Reduction	46
4.4	Biomimetic Analysis	47
	4.4.1 Brainstorming.....	47
	4.4.2 First Cut.....	47
	4.4.3 Initial Round of Questions.....	48
	4.4.4 Second Round of Question.....	48
	4.4.5 Weighting System	49
	4.4.6 Flow Chart for Biomimetic Design	50
5.	EXPERIMENTAL RESULTS.....	51

5.1	SMA Testing	51
5.1.1	First Batch	51
5.1.2	Second Batch	55
5.2	Auger Testing	58
5.2.1	Torque Requirements	58
5.2.2	Push Test	59
5.2.3	Pull Test.....	60
5.2.4	Colored Sand Experiments	61
5.3	Customized Auger	63
5.3.1	Plain Sand Experiments.....	63
5.3.2	Sand Mixture Experiments	64
5.3.3	Compacted Sand Mixture Experiments.....	65
5.3.4	Torque Requirements for Customized Auger.....	66
5.4	Vehicle Experiments	66
5.4.1	Earthworm Concept.....	66
5.4.2	Friction Reduction	67
5.5	Biomimetic Analysis	69
5.5.1	Weighted Results.....	69
6.	DISCUSSION.....	71
6.1	Shape Memory Alloys.....	71
6.2	Auger Testing	72
6.2.1	Conical Augers	72
6.2.2	Helical Augers	73

6.2.3	Custom Auger.....	74
6.3	Vehicle Experimentation	75
6.3.1	Earthworm Concept.....	75
6.3.2	Air Hose/Friction Reduction	75
6.4	Biomimetic System	76
7.	CONCLUSIONS.....	78
7.1	Shape Memory Alloys.....	78
7.2	Augers	79
7.2.1	Conical Augers.....	79
7.2.2	Helical Augers	79
7.2.3	Custom Auger.....	80
7.3	Biomimetic System	81
8.	RECOMMENDATIONS FOR FUTURE WORK	83
	REFERENCES	85
	APPENDICES	90
	Appendix – A: Draft CAD Drawing of Conical Auger	91
	Appendix – B: Auger and Motor with Fin Design.....	93
	Appendix – C: Extended Auger	95
	Appendix – D: Draft CAD of Custom Auger	96
	Appendix – E: List of Initial Question.....	97
	Appendix – F: Scenarios for Weighted Values	99
	Appendix – G: Biomimetic Flowchart.....	100
	Appendix – H: SMA Spring Data	101

Appendix – I: Final Results for all Creatures	103
Appendix – J: Information Found for Each Creature	104
Appendix – K: Metric Results for the Townsend Mole	106

LIST OF TABLES

Table 1	SMA Conversion Efficiency of the First Batch of Springs	51
Table 2a	Initial Observations of a SMA Spring at Low Currents and Loads.....	56
Table 2b	Second Testing of a SMA Spring at Low Currents and Loads.....	56
Table 3a	Digging Results of Plain Sand Experiments.....	63
Table 3b	Estimated Digging Energy of Plain Sand Experiments	64
Table 4a	Digging Results of Sand Mixture Experiments	65
Table 4b	Estimated Digging Energy of Sand Mixture Experiments	65
Table 5a	Digging Results of Compacted Sand Mixture Experiments.....	66
Table 5b	Estimated Digging Energy of Compacted Sand Mixture Experiments ...	66
Table 6	Torque Requirements of the Custom Auger	67
Table F-1	Weighted Values for Three Scenarios	99
Table H-1	Results of Spring 1 with 44.5N at Various Currents	101
Table H-2	Results of Spring 2 with 44.5 N at Various Currents	102
Table H-3	Results of Spring 3 with 26.7 N at Various Currents	102
Table I-1	Final Results for All Creatures	103
Table J-1	Information Found for Each Creature.....	104
Table K-1	Metric Results for the Townsend Mole	106

LIST OF FIGURES

Figure 1 - Hysteresis Loop in Shape Memory Alloys [18]	13
Figure 2 - Testing Platform	28
Figure 3 - Machined Attachment Connecting the Conical Auger to the Motor	31
Figure 4 - Motor with Attached Rod for Counter Rotation	32
Figure 5 - Coupling Devices Connecting the Helical Auger to the Motor	33
Figure 6 - Adaptor Connecting the Helical Auger to the Motor	34
Figure 7 - View of Augers Tested	35
Figure 8 - View of Aluminum Rods used for Push Test	37
Figure 9 - View of Pull Test Pulley System	39
Figure 10 - Multi-Colored Sand used to Examine the Auger Sand Interaction	40
Figure 11 - View of Auger Designed by UMR	42
Figure 12 - Diagram View of Earthworm Design	46
Figure 13 - Graphical Representation of the Current vs. Stroke Results	54
Figure 14 - Graphical Representation of the Force vs. Time Results	55
Figure 15 - Graphical Representation of the Depth vs. Torque for Various Augers	59
Figure 16 - Graphical Representation of the Results from the Push Test	60
Figure 17 - Profile of Digging Trial using a Sand Core	62
Figure 18 - Stopping Point of the Earthworm Digging Trials	68
Figure 19 - View of Motor with Air Hoses	69

Figure A-1	Side and Top View of Conical Auger.....	91
Figure A-2	Cutaway View of Conical Auger.....	92
Figure B-1	Motor with Three Small Fins.....	93
Figure B-2	Motor and Conical Auger with Two Large Fins.....	93
Figure B-3	Motor and Conical Auger with Rod Fin Design.....	94
Figure C-1	Extended Auger used for Pull Test.....	95
Figure D-1	Side View of Custom Auger.....	96
Figure G-1	Biomimetic Flowchart.....	100

1. INTRODUCTION

Screenwriters and storytellers conjure up fairytales about self thinking and self assembly robots that wreak havoc and destruction upon mankind in order for machines to gain their freedom and eventually rule the world. Although this scenario is still far from becoming reality, science and technology advances every generation, from the invention of automobiles to ease travel on the ground to the birth of aviation, which enables us to soar through the air. When ground and sky were no longer enough, space travel opened up a much wider and more complex playground for us to explore. However, while all these things have helped mankind become faster, stronger and better, a new wave of technology has grown to be part of our lives: remote control. Mankind can now reap the benefits of older inventions, but without having to be physically present atop the machine. Today, those same machines that were originally remotely controlled are now being upgraded to give them the capacity for what might very loosely be described as “intelligence”. Autonomous vehicles are being created that are capable of covering ground, air and sea.

Large earthmoving machinery has followed the same progression. Today’s machines have sensors and computer controlling devices instead of human operators that enable them to react with the surrounding environment [1]. Large amounts of earth can be moved with these machines, but not without overcoming large forces. Instead of moving the earth out of our way, why not move through the earth?

Augers are widely used in the construction industry to accomplish simple tasks, such as post hole digging, or even large tasks, such as drilling roadways through mountains or under rivers. An auger's design is intended to break up the material and transport it out of the way, hence moving within the earth and moving the earth, simultaneously. Unfortunately, these uses require power supplies that are more substantial than a few AA batteries and forces larger than a few Newtons.

A closer look at Mother Nature reveals that insects and some mammals have no problem moving within the earth. They need no large power supplies or (at least in some cases) hours of work to travel distances of five or even ten times the length of their bodies. What is it that gives these creatures the ability to dig so effectively at depths that are many, many times their own size?

Just as autonomous vehicles in the sky, sea or on land have their own unique functions and capabilities, an autonomous digging vehicle has the potential to be used in many real world applications, such as civil search and rescue missions, geological exploration on earth and other planets, and industrial uses such as drilling air vents for mine shafts or wire and cable emplacement for construction projects or data transmissions.

This thesis consists of a study of three different approaches to designing an autonomous digging vehicle, namely the possibility of creating one through the use of shape memory alloys (SMA), augers, or new techniques inspired by Mother Nature's own creations. The project originally intended to have the vehicle move through a given medium, in this case sand, through the use of shape memory alloys. This metamorphosed into the possibility of a vehicle constructed of a motor and auger. The final phase

involved a literature study and observant evaluation of several creatures and their different digging techniques in order to examine how their physical characteristics contributed to their outstanding digging performance.

2. LITERATURE REVIEW

2.1. History of Drilling

Since the earliest days of pre-history, mankind has drilled holes in the earth's crust. Drilling equipment and needs, from today's standpoint, can be grouped into different categories based on the specific needs of different industries, such as those associated with gas, oil or mineral exploration, construction and excavation or quarrying and mining [2]. However, in ancient times, the main need was to find a source for water and some of the best-preserved structures from ancient civilizations are water wells. One example, dug in ancient times, is located in Cairo, Egypt and is named "Joseph's Well" [3]. With a total depth of about 90 meters (295 ft) and traditionally powered by oxen pulling on long chains with buckets attached, records show it to have produced water right up until the year 1900 [3]. An early European well, located outside the village of Lilliers in northern France, was drilled in 1126 A.D. and still produces water to the present day [3]. One of the oldest forms of drilling dated back around 600 B.C. when the Chinese developed a technique that is now called percussion drilling [4]. Chung, [3] describes the early process as a spring pole, tapered on one end, being placed on a fulcrum, giving the effect of a lever. A heavy weight is placed on the thick end and the drilling tool is attached by rope to the tapered end. A hollowed piece of wood is placed in the ground, directly beneath the cutting tool to provide stability to the borehole and guidance for the cutting tool.

A group of two men then lifts and lowers the cutting tool inside the log, with the help of the fulcrum, giving the tool a spin with each strike to make sure the bore hole is even and symmetrical. This work continues day and night, for many years if necessary, until the final depth is reached. Another form of drilling, rotary drilling, was used as far back as 3000 B.C. by the Egyptians [5]. Here, a sharp edged flint is attached to one end of a forked stick. The tool is then spun into the bore-well with the leverage of the forked end. Helical grooves can be seen along the walls of the boreholes produced using this method [3]. Both percussion and rotary drilling are still used in modern times, although the materials have advanced for percussion drilling, with the spring pole and rope being replaced by steel pipe and chains and the striking against the ground has become automated with the use of gears and machines. A French engineer named Leschot [6] developed the first modern rotary drill around the 1960s. Constructing a tunnel for a railway system linking Modane, in France, and Bardonecchia, in Italy, Leschot built a belt driven rotary drill with a black diamond face [3, 6]. Percussion drilling was used for oil drilling in the early days of the oil industry, although it was eventually replaced by rotary drilling in the 1930s due to the faster rotations that were possible. Before the 1930s, speeds of only 30-60 rpm could be maintained but with the introduction of diamond bit sets, speeds increased dramatically to 200-400 rpm [3].

2.2. Earthmoving Equipment

One of the leading industries that makes extensive use of earthmoving equipment is construction. There will always be a demand for bigger and better skyscrapers and bridges, and hence a need for bigger and better earthmoving vehicles. It is not the vehicles that move the earth but the cutting tools attached, which in the case of bulldozers

and power shovels takes the form of a scoop or bucket. Experiments designed to optimize excavator buckets have tested everything from the width of the bucket to the number of teeth and the spacing between each, the length and position of the teeth or buckets with no teeth at all [7]. Maciejewski et al. [7] concluded that the total amount of work done increased as the number of teeth increased and stabilized upon reaching a high number of teeth. These types of fundamental experiments are being performed in order to provide a better understanding of a soil's behavior. Experiments have shown that the initial conditions (blade geometry, soil type) and the operating conditions (cutting speed and depth) have a significant effect on a machine's productivity [8].

Doing field experiments can be tedious and expensive over a period of many trials, but the use of Finite Element Analysis (FEA), can help ease this burden. FEA simulations have the advantages of not depending on the accuracy of measuring devices, as in physical experimentations, replicating more sophisticated material phenomena and revealing details of the soil-blade interactions [8,9]. Simulations can be set up with different variables, such as cutting speeds and depths that are not limited by the available machinery and space. However, the limiting factor for FEA models is the computational power, as an increase in mesh density causes a considerable increase in computing time and power [10]. Many models are being investigated, although there is some difficulty in providing realistic estimates of soil strength. Some research, like that of Georgiadis et al. [9], are helping to validate the empirical models for soil shear strength by comparing the failure models with experimental results.

Another focus on earthmoving equipment has been to optimize the vehicles themselves. The approach generally taken has been to provide a continuous monitoring

system to assist the operator. However Maciejewski and Jarzebowski [1] are attempting to develop an automated vehicle whereby the vehicle can react to soil conditions and optimize the earth-working process. Again, by experimenting with the shape and trajectory of the excavating bucket they concluded that the digging method of cutting thin layers of soil, as performed by bulldozers, is inefficient as this method involves a higher energy dissipation per unit volume when compared with other digging methods.

To help reduce the need for bulky earth-moving equipment, the use of trenchless technology is greatly increasing. The gas line industry has invested considerable research time to developing better vehicle designs specifically for directional drilling and trenchless technology [11]. With increasing worry over environmental issues such as animal habitat impact and disruption, directional boring vehicles offer many advantages compared to conventional earthmoving vehicles (bulldozers, cranes, scrapers) [12]. These machines are more cost-effective as the space and time to set up is minimal with a corresponding increase in work productivity, maneuverability and number of bores per day [11].

Research has also increased the capabilities of tunnel boring machines or TBMs, which are primarily used to drill tunnels in hard rock [13]. These machines are now successfully drilling in ground and rock conditions that were thought to be impossible years ago. The first TMB built in the United States was in 1856, although “neither metallurgy nor structural design were to the point where it could be successful in hard rock” [13]. However, technology has come a long way and today TBMs are very cost effective due to their ability to apply a relatively constant power, gather up the cuttings and convey them to a haulage unit. With today’s emphasis on safety when tunneling,

TBMs offer improved overhead protection during operations, creating smooth walls for a more stable opening and fewer collapses [13]. In terms of automation, TBM companies are experimenting with laser guidance to help in automatic steering [13,14]. By incorporating sensor systems, TBMs are also beginning to gain an ability to respond to changes in rock and ground conditions in order to establish an optimum machine performance and thus allow for maximum penetration [14]. As with all large vehicles, a smaller version may often be needed for different scenarios, hence the creation of small boring units or SBUs. SBUs were developed in part because sometimes the size or cost of TBMs prevents their use. SBUs can be used for smaller jobs such as ventilation tunnels or man-ways in mining [14,15]. Being smaller, they can also be steered more readily. One such development by a Japanese contractor has created a TBM that can make a 90° turn. This particular model creates its own access shaft, which not only shaves months off the time needed, but may also cut the project costs by as much as 15% [15].

2.3. Augers

For the geological surveys required for constructing roads and large building complexes, soil sampling is a large-scale operation and with the new demands of space exploration, extra-terrestrial soil will be the next step. Soil sampling consists of collecting samples from below the surface to help identify changes in their characteristics. Augers have been used for this purpose for decades, although their earliest uses were for wood working. Augers come in many different sizes, ranging from small hand held tools to large augers that are anchored on the back of trucks. Augers are designed with spiral flights to keep material moving to the surface and hence do not

require a continuous flushing medium to keep debris clear of the cutting tip. Research by Sellmann and Brockett [2] has shown that a well designed auger bit can operate effectively in many different materials, as long as the necessary torque and thrust is applied, although some augers are designed for specific applications. However, some disadvantages when using augers for drilling in harder materials are rapid bit wear and the large drill rig needed to provide enough thrust for holes nine inches or larger in diameter.

As the National Aeronautics and Space Administration (NASA) pushes forward to explore our solar system and its planets, drilling and excavation technology will be a vital tool. “To date, drilling has only been conducted on the moon to the depth of a few meters and on Mars to depths measured in centimeters” [16]. Research and testing is underway, sponsored by NASA, for a tethered hole drilling system to help overcome these limited depths. The grinding motion or shearing action of a cutting tool accomplishes the majority of rock cutting or down-hole drilling processes and a large thrust and/or torque is usually required, also known as “weight on bit,” to keep the cutting tool continuously moving [16]. This is accomplished by anchoring the drilling mechanism above ground or, in the case of oil drilling, the weight on bit is self-provided by the weight of the drilling unit, which incorporates long tool strings. Hill’s group [16] has developed, a Low Reaction Force Drill (LRFD) to address NASA’s needs, which consists of a “detached, self-driven underground autonomous tethered drill system”. Some of the advantages of the LRFD are its low energy requirements, unlimited depth capability, and the ability to self-advance, which are all self-contained [16]. This requires less equipment and a correspondingly lower mass to transport, a major asset for NASA

when considering the enormous cost of lifting equipment out of earth's gravity well. The LRFD uses a cutting bit at the tip of the device with multiple augers or helical flights acting as cutters to advance the drilling system [16].

2.4. Revolutionary Drilling

Along with augers, diamond bits and other traditional drilling devices, researchers are designing and testing new methods to dig deeper and faster than ever before. One such method is not new, but has simply become more feasible with the advancement of technology, namely lasers. In laboratory tests, lasers were aimed at pieces of sandstone and were able to cut through a 150 mm specimen in four seconds, ten times faster than rotary drills [17]. However, as rapid as lasers are, they also require a large amount of energy and would not be very efficient in large hole operations. Another method being tested by the U.S. Department of Energy is thermal spallation [17]. Thermal spallation uses a heat source to quickly heat a rock so fast that it expands and explodes into small pieces. Heat sources being experimented with include electric arcs, microwaves and simple flames. The disadvantage is that spallation is limited to rocks with large crystals that fracture cleanly [17]. One of the more interesting methods is a mechanical device that melts its own way down. Named the subterrene, this device is a large electrical resistor with a cone-shaped ceramic tip. The disadvantage is its limited speed of about one meter per hour [17].

2.5. Shape Memory Alloys

Shape Memory Alloys (SMA) are alloys that experience a Shape Memory Effect (SME) due to phase transformations. Discovered in 1932 by Swedish physicist Arne Olander [18], the SME behavior was observed in a gold and cadmium alloy that could be

plastically deformed at cool temperatures and then be promptly returned to the original shape through the application of heat.

Shape memory alloys are constantly being sought, with about a dozen already proven. Materials experience the SME due to a “temperature and stress dependent shift in the material’s crystalline structure between two different phases called martensite and austenite” [18]. Most SMAs are thermoelastic in that it can be plastically deformed when at temperatures below the transition temperature and recovered when heated to temperatures above the transition temperature. A shape memory alloy’s capabilities are due to a solid-state phase change in the material; “a martensitic – austenitic phase transition - and at low temperatures – to martensitic twinning” [19]. At lower temperatures the material is found in a twinned martensitic state. With an applied stress the material can be deformed in which the martensite twin variants shear into a parallel orientation [19]. After removal of the stress, the structure remains until the material is heated, in which the sheared twins revert back into the organized austenitic phase. Upon cooling the martensitic twins form again, completing the SME cycle. Austenite’s cubic structure and un-deformed martensite’s twinned structure are the same size and shape on a macroscopic scale resulting in no change visibly [19, 20]. In contrast to this process is an SMA that is designed to work using superelastic behavior, that is, a stress induced martensitic formation [20]. Through changes in alloy composition and heat treatment, an SMA’s phase transformation temperature can be manipulated [20,21]. By controlling this temperature to be slightly below room temperature, the SMA will be in its parent austenitic phase even when no load is present. When a load is applied however, a martensitic transformation will occur. Because martensite has formed above its transition

temperature, if the load is removed, the new phase becomes unstable and reverts back into the austenite phase and again, the original un-deformed shape is recovered. This is different from SMAs that have a transition temperature above room temperature because no temperature change is necessary for the material to recover its original shape [19,20,21]. SMAs are typically heated up using one of two ways, either electrical current (resistance heating) or with a high temperature medium surrounding the material such as air or water [22].

SMAs were first used as fasteners that functioned as coupling devices for piping systems and electrical connections [20]. Later, research focused on using the alloys as actuators for temperature-regulated systems such as greenhouse windows, automobile fan clutches and air conditioners [23]. Recent research has examined their use as actuators for micro-robotics. Conventional actuators, such as DC, pneumatic and hydraulic motors, are not energy efficient due to their large volume and heavy mass [18]. SMAs have an advantage over these through their high force to weight ratio [18], high power density, large stress and strain [23] and noiseless operation capabilities [18], although, the actual electrical energy to mechanical work conversion can be very inefficient with SMAs.

The main disadvantage for SMA applications is the cooling required. For large actuation forces, larger SMA wires are needed, requiring larger power demands to heat and, in turn, a longer cooling time. The dominating factor in a cycle is the cooling time. An SMA cycle follows a hysteresis loop (figure 1). Starting at point 1, the material is completely martensitic at temperature M_F . Following the bottom curve, the temperature increases and austenite starts to form at temperature A_S . Further heating transforms the

microstructure to complete austenite (A_F), at point 2. Upon cooling, the material follows the upper curve, in which martensite starts to form upon reaching temperature M_S and completes the loop, cooling back down to the 100% martensite microstructure at point 1.

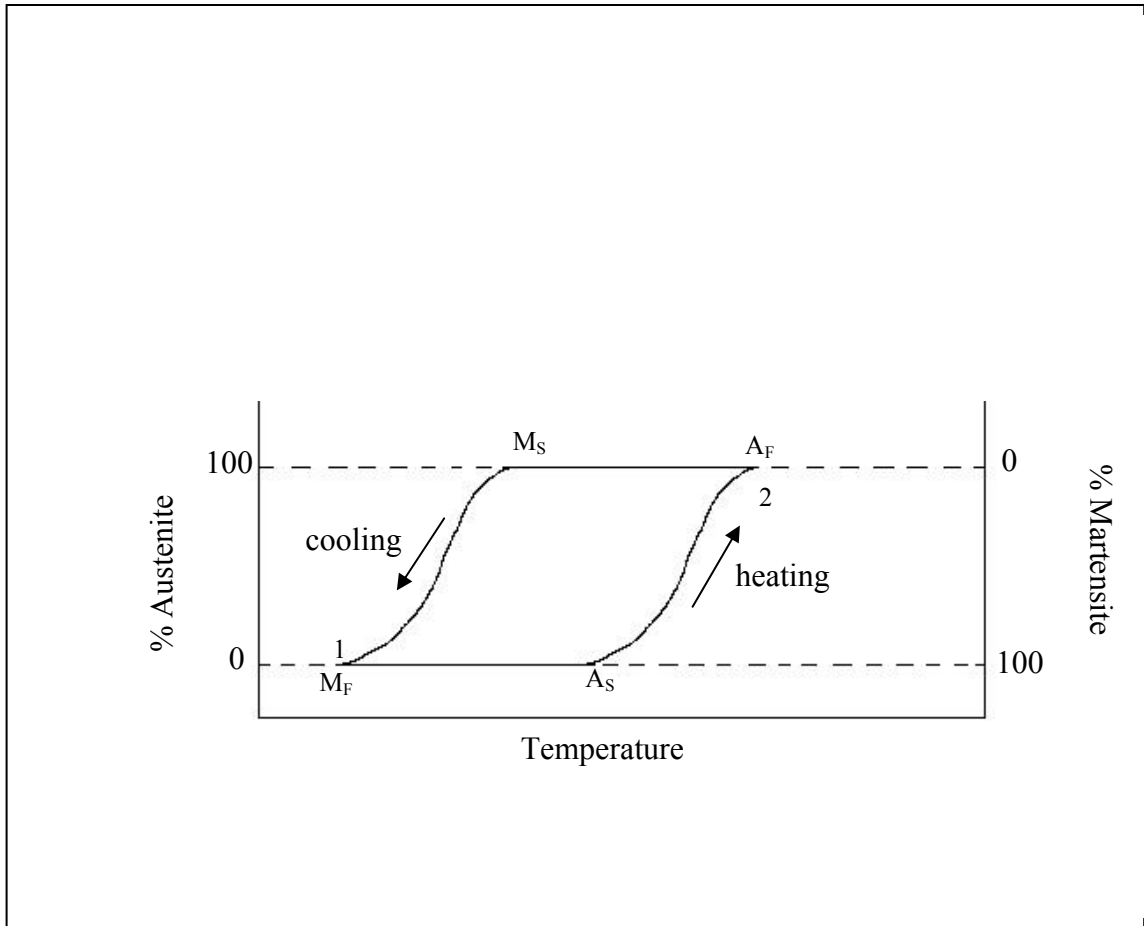


Figure 1. Hysteresis loop in shape memory alloys, after Mavroids et al. [18].

2.6. Mechanical Biomimetic Devices

Biomimetics is not a new field of science, but simply a new name given to help identify a particular engineering concept. In fact, science has tried to replicate nature for hundreds of years. Simply, biomimetics is the ability to apply biological concepts to engineering processes or systems.

In the mid 1400s, Leonardo da Vinci drew sketches of flying contraptions based on the flight habits of birds [24]. However, it was not until the 1800s that the visualization of da Vinci's drawings became reality with the construction of ornithopters [25], which were flying devices. Again based on the flight of birds, these mechanical devices had large feathered wing-like structures on both sides, powered to flap under the control of the human pilot. Unfortunately, these devices quickly proved that there is more to flight than just wings flapping; birds are at ease with the motion due to their size/weight to wing span ratio. When undertaken on a scale sufficient to lift a man and machine however, the concept proved to be unworkable [25].

During the 1950s, an avid hiker by the name of George de Mestral noticed small "burrs" that clung to his pants and his accompanying dog's coat. A closer inspection under a microscope revealed that the burrs had small, stiff, hooks with which they could grab onto the looped fibers of his clothes and his dog's hair. From this observation came his invention of Velcro, whose name originated from combining the words velour and crochet [26].

In the 1990s, high performance swimsuits were introduced that mimicked the skin of sharks. This concept was based on observations of a reduction in the number of eddies in the water flow along the surface of the shark's skin as it moved through the water. The result was to copy the v-notch pattern and apply it to full body swimsuits. This design is believed to reduce the drag encountered while swimming by up to 8% [27].

One of the most well known biomimetic devices is the MIT RoboTuna, built by then Ph.D. candidate David Barrett in 1995. This research focused on developing and studying a better propulsion method for underwater vehicles [28]. By mimicking the

fastest fish – the blue-fin tuna – the group at MIT hoped to control the vortices encountered while moving underwater. Normal vehicle movement, due to a screw or propeller is slowed by these vortices, and generally designers aim to eliminate them. However, fish intentionally cause and control with their fins these vortices to boost their speed. Besides increased speed, the RoboTuna can operate at greater depths than most Autonomous Underwater Vehicles (AUV) because the skeletal structure does not require a pressurized chamber. This will not only be beneficial in the study of thermal vents along the ocean floor, but also for other dangerous explorations or even search and rescue missions that maybe undertaken in the near future.

Autonomous vehicles are currently a major focus for science and industry, with the Department of Defense leading the way in spending. The Robotics Institute at Carnegie Mellon University has seen its federal funding more than double since 1994. Other well known technology based universities have also seen a 50% increase in just the last few years [29]. Some see a robotic nation in the near future and with the way the Defense Department is spending, the idea is not so far fetched. The Pentagon is thought to have spent \$3 billion on Unmanned Aerial Vehicles (UAV) between 1991 and 1999, with an estimated budget of \$10 billion through the next 5-6 years [30]. In 1946 it was revolutionary to fly two, unmanned B-17 bombers from Hawaii to California by remote control from the ground, yet in 1999 when a completely computer controlled UAV flew itself across the Pacific to Australia where it landed perfectly [31], this feat was not considered revolutionary but rather expected, due to the natural progression of technology. UAVs are not only confined to airplanes; unmanned helicopters are also being developed. A group at MIT has developed a small, agile and acrobatic helicopter

that they expect to be widely utilized. The main driving force for this rapid development is for military applications, namely reconnaissance, weapons delivery in mountainous, urban or other hazardous regions, low altitude or tight spaced missions, all of which can send images to a remote location or to an aircraft already in flight. Along with military applications, the MIT design group expects the helicopter to be used in surveying disaster sites or even filming aerial views for motion pictures [32].

The Defense Department is pushing for one-third of its ground vehicles to be unmanned by 2015 [30]. With this comes a challenge to industry and academia to produce the technology needed to control Autonomous Ground Vehicles (AGV). The Defense Advanced Research Projects Agency (DARPA) has issued a challenge with a grand prize of \$2 million to the team that can produce an unmanned ground vehicle capable of tackling different terrain and obstacles on its own. Held annually, DARPA hopes to “accelerate research and development in autonomous ground vehicles that someday will help save lives on the battlefield” [33]. In 2005, only 25 of the 86 groups that applied were selected to participate in the event, and only 15 of these were allowed to proceed after initial qualification, inspection and demonstration stages. However, so far no vehicle has successfully navigated the complete course and the prize remains unclaimed.

2.7. Wildlife Research

Overall, about 40 different creatures have been investigated by this project team, in terms of their digging capabilities. Many share the same digging approach, however some distinguish themselves due to their absolute and relative tunnel lengths.

Marine creatures are not the first subjects to come to mind when looking for a natural digger to model an autonomous vehicle after. Some creatures, such as the razor clam, have an advantage compared to those on land because of the nature of their digging medium. The razor clam forces its foot-like muscle into a soft substrate, in this case sand, and uses the “foot” as an anchor by filling it with blood and expanding it. Once secured in the sand, the muscles pull the shell down to the foot. The two halves of the shell expand, compacting the surrounding material and the steps are repeated until the clam is safe from harm. The razor clam can bury itself quickly, in as little as 15 minutes [34], compared to the geoduck clam, which digs in the same manner but can only dig a total of about 910 mm (36 in) in a period of three years [35]. Boring Clams take a harder path to security as they bore into something more stable, such as living coral. After the clam secures itself to a hard substrate, an acid is released to break down the carbonate in the coral and the two shells start to grind away, slowly making an entrance [36]. The so-called shipworm, which is actually a mollusk, is a relative of the boring clam family in that it also has small rigid shells that it uses to grind away material; however, here wood is the primary source instead of rock. The shipworm gains nutritional support from the wood substrates as well as protection. The tunnels remain open due to a calcium secretion along the tunnel walls [37].

Insects have also become a resource for those studying burrowing mechanisms. The problem is to find a true burrowing insect, as opposed to one that digs as a nymph for protection to carry out the remaining of its life cycle. One true burrowing insect family is the mole cricket. Because of the damage caused by the mole cricket, a group at the University of Florida has devoted a lot of time to researching and observing the mole

cricket specifically. These small insects, related to crickets and grasshoppers [38], have large paws as nymphs and adults that are essentially replicas of those found in mammals. The family can burrow with ease through sandy soils by parting the soil with their large claws, much as a mole would, and feed on the plants and grassland. An entire database is devoted to these creatures [39]. The dung beetle is another insect that is a pure digger. The dung beetle is actually a family of beetles, as there are thousands of species. These are an example of an environmentally friendly insect, feeding off the dung of animals. By extracting the liquid from the dung, the insects satisfy all of their nutritional needs including water [40]. The beetles can then roll up the remaining material and bury this to provide a habitat for their young. Most species of dung beetle, however, dig tunnels underneath the dung pile and bring sections of it down into the tunnels [41]. Many insects, such as the June bug or cicada, will bury themselves as grubs (a younger stage in the life cycle) and stay buried for months until they mature into an adult. The motion is that of a wiggle as their bodies squirm back and forth in the material until a satisfactory depth is reached, usually sufficient to keep them warm during the winter. The insects mentioned so far are of a solitary nature, however the termite is well known for the large numbers found in each colony. It is not known if termites work together in a coordinated fashion or if they randomly dig together. Termites are renowned for their wood eating abilities and live in large colonies underground, up to 5.5-6.0 m (18-20 ft) below the surface [42], or in large dirt mounds found above the ground. The workers have large heads with massive pincers that they use to tear off pieces of wood or carry grains of soil. An interesting creature that digs in its own unique manner is the trapdoor spider. This particular spider creates burrows for protection, a place to mate and a place for their

offspring. They loosen soil with small, hard, spike-like hairs attached to muscles called rastellum [43]. These spiders are able to maneuver the rastellum back and forth against the soil, breaking up small amounts at a time. They then remove the soil in one of two ways, either by pushing the loose soil out with their legs or by forming clumps of soil that are wrapped in silk and carried out as a package. The burrows protect the spiders from temperature fluctuations, flooding and caving in due to a silk lining around the walls.

One amphibious creature that burrows is the Mexican burrowing toad, which prefers areas with loose soil [44] and digs by using the spades found on their powerful legs [45]. However, there is no information available on the exact motion used to burrow with their spades.

The bulk of the research in this area has come from mammals, specifically families of rodents, such as squirrels, gophers and gerbils, moles and mole rats. Rodents dig in the usual manner, with their legs in the front of their body. Some, like the plains pocket mouse and the yellow cheeked vole, live in shallow burrows of 0.30 m (12 in) [46] or less while others, for example the olive backed pocket mouse and Malagasy Giant rat live in burrows that reach down 2 m (79 in) [47] or deeper. The only difference between the many burrowing squirrels and gerbils is the depths of their burrows.

Gophers are highly fossorial and have bodies built for their living style, with “thick, tapering bodies, short limbs with strong claws, loose skin, and reduced eyes and ears” [48]. They also have large and ever-growing incisors, which they use to scrape at the soil to loosen it up. After a considerable amount of soil is accumulated, they hold it with their forearms against their chest and push it out to the surface with their bodies [49].

Mole rats are a social group living in colonies that coordinate their effort when creating burrows. They have tiny eyes that can detect light and nothing else, a wide and flat head and, like gophers, large incisors that are used to scrap at the soil. The lead mole rat will loosen the soil with its teeth and then push the loose material underneath and behind its body with its feet. A train of mole rats behind the lead digger will then continuously push the material up and out of the tunnel to the surface by passing it to the next mole rat behind them. In the naked mole rat, 25 % of their muscle mass is located in their jaw [50], enabling constant digging with their teeth.

The most impressive digging animal is the mole, as both its claws and body are highly adapted for burrowing. The forelimbs of the mole are located to the sides of its body, instead of in front, and are pointed outward, as if ready to swim through the soil. The mole's humerus bone and muscle structure is uniquely adapted to allow the forelimbs to rotate in this manner while combating the forces encountered as they push the soil away from the body. Their bodies are almost cylindrical, as well as streamlined. Like the gopher, the eyes and ears are small, forming a robust and solid skull. The claws on the forelimb are as wide as they are long, forming a "broad and shovel-like" [51] structure that is well suited to moving the excavated material.

2.8. Autonomous Technology

2.8.1. Power Supply

The provisions of an autonomous vehicle power supply is an on going challenge in optimizing the balance between the amount of power required to function and the sustainability of the battery to allow it to run for long periods. Unless they are tethered to an external power source, self-powered vehicles are limited in the amount of power

carried by the overall size of the vehicle and the determining size of miniature robots is limited by the size of the power source [52]. As Sandia National Laboratories researcher Doug Adkins observed, the “batteries need to run longer and smaller” [52]. Three watch batteries are used to drive his 41 cubic millimeter autonomous self-powered robot. “Low power processors and electronic tricks” helped Francesco Mondada and his research team at the Swiss Federal Institute of Technology in Lausanne, Switzerland to achieve the necessary power requirements to power their SWARM-BOT [53]. Like Doug Adkins’ problems with miniaturization, complex mechanics and powerful electronics rapidly drain the energy available to propel the device. The SWARM-BOT uses two lithium-ion cells to power the vehicle in standard operation; however power is saved by programming the processors to hibernate when not in use. A group headed by J.M. Kahn assembled a smaller package by developing a self-powered vehicle through MEMS technology. Called Smart Dust, this team from U.C. Berkeley is developing a vehicle that has the ability to sense and communicate, powered by solar cells, all in the space of a cubic millimeter [54]. In an attempt to avoid power consumption from on-board power supplies completely, some research groups are powering individual mechanisms and/or functions with separate power supplies [52]. It is suggested that the latter route should be followed with a digging vehicle. The use of two power supplies would help to maximize the efficiency; with a deep draw cycle for powering the vehicle during digging and a light duty cycle after the final depth is reached and surveillance and/or communication is necessary.

2.8.2. Single Vehicle vs. Group Approaches

Research has expanded from developing a single autonomous vehicle able to handle multiple tasks to designing a range of autonomous vehicles able to perform specific tasks individually or as a group effort [53,55-60]. Robustness, reliability, efficiency, all-terrain capability, flexibility and adaptability are all important when building autonomous vehicles [53,56-60]. One of the ways to incorporate these qualities is to develop a group of vehicles that act as a unit, and this strategy has been titled “Swarm” technology [60]. From planetary exploration [52] to the ability to connect together as a single unit [53], the inspiration for the concept has come from the many social organizations found in Mother Nature.

There are many advantages to swarm technology, with the biggest being the ability to continue a mission in spite of the loss of one or more of the members of the swarm, characterized as robustness. In a single robot, programmed for many tasks, if any part of the robot fails, the mission correlating to that function has been lost. However, in a swarm, if the same scenario occurs, another robot can complete the mission. Currently, there is much discussion as to whether it is better to develop many simple separate tasked robots [53,56,58,60] or to create many robots that all have the same capabilities [54,61]. In the case of exploration, it would be logical to disperse many vehicles that are capable of the same functions [55,61], especially when dealing with power supply issues. The larger the area covered in a given time, the better. Another benefit is the decrease in cost when mass-producing multiple robots. Instead of developing a high-tech, one-of-a-kind robot, it may be more cost effective to produce many simpler robots. The question then is, how do the members of the swarm communicate with each other?

2.8.3. Communication

Swarm communication has been inspired by many fields, but primarily ethology, or the study of animal behavior. From the pheromones produced by bees and bee dances [62] to the indirect communications observed with ants [58,63], the ability to communicate in some manner is necessary or else efficiency is decreased [55,60,63]. There are many possibilities when trying to develop communication within a swarm. One option is to use centralized control, with a main robot controlling others, while the main alternative is decentralized control, with each robot able to govern itself based on its programming and/or communication throughout the swarm. However, centralized control has been proven to lack robustness. If the main unit fails in any manner, then the rest of the swarm ceases to function due to a lack of orders. Information received by the main unit can also become excessive with an increase in the number of units in the swarm. As each robot transmits information to the main unit, then a bottleneck can occur, causing some information to be fragmented and lost altogether. A more flexible and robust method is to decentralize the group, although there are various options within this scenario. One question is whether the robots talk to the entire swarm (global) or to specific neighbors (local)? Another possibility might be not to communicate at all, but simply to proceed based on the prevailing environmental conditions. Kube and Bonabeau [58] successfully attempted this for a group of autonomous vehicles cooperating in a specific assignment of moving a box. Based on the implicit communications of ants, the robots can sense the forces upon the box and decide whether it is helping or hindering the effort. If it is helping, it continues with the process,

however if a robot realizes that it is hindering the effort of the group then it will reposition itself until deemed helpful, by its own judgment.

3. RESEARCH OBJECTIVES

The original objective of this project was to design a vehicle that could dig through soil using a mechanism based on the mechanical action of Shape Memory Alloys (SMAs). However, the small size of the SMA springs required many springs to be used, both in parallel (for force multiplication) and series (for stroke multiplication) with each other, in order to generate sufficient force and stroke. The time needed for cooling between cycles was also a major issue. Increasing the size of the springs might lead to needing fewer springs and having the ability to move at greater lengths per heating/cooling cycle, but would also increase the time needed to reach the austenite temperature and the time to cool back down for a repetitive cycle. Testing revealed that larger springs suffered from “memory loss” (what is sometimes referred to as “shape amnesia”) at high currents, resulting in permanent deformations of the springs and they were thus deemed not suitable for this application.

The project then moved on to consider the use of augers in conjunction with a small motor to create a digging vehicle. Various sizes and shapes of augers were researched and tested. The limiting factors for the design were found to be the size of the motor, the size of the auger, the nature of the coupling device and the amount of power that could be transferred to the auger. Large augers created too much force for the motor to overcome, halting the descent, while smaller helical augers suffered from problems due to the devices used to couple them to the motor. An auger designed specifically for

digging in sand proved too large for the available motor to handle. As a result of the design flaws and failures experienced during the tests of shape memory alloys and augers, it became clear that a new approach is needed. A look at the results of nature's design process through examining the techniques used by fossorial creatures may inspire new designs for digging vehicles. The preliminary study performed for this thesis may provide the basis for the selection of a creature for further study as a possible basis for a radically new strategic and scientific approach to developing a digging vehicle.

4. MATERIALS AND METHODS

4.1. SMA Testing Procedure

In previous years, tests performed by Dr. Daniel Butts and Dr. William Gale demonstrated the effective use of SMA springs as actuators for digging devices. However, due to the small size of these springs, many were needed in series and parallel to move the digging device. The effort to manufacture springs that can produce a larger force than the existing prototypes required collaboration with an outside source, Shape Memory Applications, Inc. The new springs were then characterized in terms of their stroke, time, force and current, over a range of values using a structure erected from metal tubing and anchored to a testing bench, as shown in Figure 2.

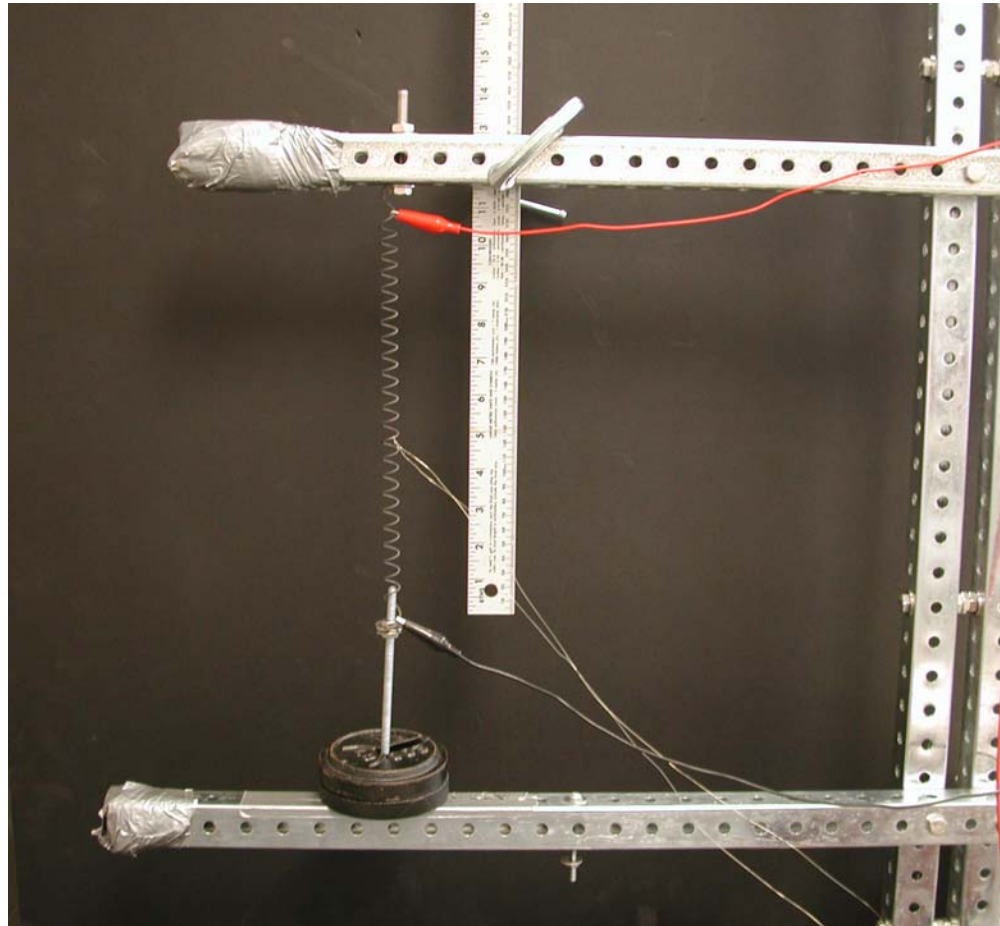


Figure 2. Testing platform.

The test structure consisted of an upper arm, to which a SMA spring with a weight was attached, and a lower arm, to prevent the spring from overextending. The spacing between the upper and lower arms was sufficient to allow the SMA spring to be stretched effectively, without harm, and could be adjusted depending on the size of the spring. One end of the spring was attached by clamping the wire tightly between two washers on the upper arm, with the opposite end of the spring attached using the same method to a weighted hanger. Calibrated cast iron weights, known as counterpoise weights, could be added to or removed from the hanger as needed. Once the spring was

stretched to the desired length, the resulting stroke distance was measured. Two leads were placed at each end of the SMA with crimp connectors. The wire was then resistance heated by using a DC power supply capable of variable voltage or current. The power supply was attached to the spring by using wire clamps.

The first batch of larger SMA wires were shape set annealed with an oxide surface, with a nominal A_f (Austenite Finish temperature) of 46.2 °C, a wire diameter of 1.17 mm (~0.05 in), a total of 27 coils and a total length of 1.08 m. Multiple tests were conducted with a fixed current and weight, recording the stroke and time for each. The current ranged from one to six amps and the weights ranged from no additional weight (weight of spring) to 22.25 N (5 lbs). The second batch of SMA wires had a larger diameter, measuring 1.75 mm (0.07 in). Because these were significantly larger, the fixed current and weight were increased. Testing started at a 44N (10 lb) load at 10 A and increased in increments of 8.9 N (2 lbs) and 2 A up to 89 N (20 lbs) and 20 A. An interval of 300 s (5 min.) was allowed between each individual test, to permit sufficient cooling of the relatively heavy gauge SMA wire.

The stroke length was determined by reading the length from the yard stick. Before the current was applied, the yard stick was aligned with the lower end of the spring (i.e. the end with the weight attached). After the current was applied and the SMA returned to its original shape, the resulting length was recorded. The time for each test was recorded using a digital stopwatch.

4.2. Auger Testing

4.2.1. Electric Motor

To provide a comparison for the SMA results, digging tests using a direct current (DC) electric motor were conducted. The research team, as a sufficient starting depth, agreed upon a 209 L (55-gallon) drum with a depth of 0.90 m (36 in) and diameter of 0.58 m (23 in). Off the shelf silica sand, dried and non-compacted, was used for the testing bed.

Testing consisted of digging in the 55-gallon drum at various fixed voltages, recording the depth reached and time for each. The power supply used in the SMA testing was also used to power the motor. The depth achieved was expressed in terms of the amount of vehicle buried rather than an absolute measured depth. The time was recorded using a stopwatch.

4.2.2. Conical Auger

Initial tests were conducted using a conical auger (see Appendix A for dimensions) designed by Rob Langley at Auburn University and fabricated by the sponsor. An adapter, designed by Daniel Butts at Auburn University and supplied by the sponsor, was used to attach the motor (also supplied by the sponsor) to the conical auger. As shown in Figure 3, the adaptor acted as a reducer to accommodate the large diameter of the auger compared to that of the motor. The plate was secured to the auger and motor with bolts and a setscrew, respectively.



Figure 3. View of machined attachment connecting the conical auger to the motor.

The digging tests used fixed voltages of 5, 10, 15 V with time and current being recorded at auger depths of quarter, half, three-quarter, and fully buried, as well as the final point of descent (i.e. maximum attainable depth). Each test was run three times, giving a total of nine digging trials.

To keep the motor stationary, different anti-counter rotation devices such as large flat fins and cylindrical rods were tested. However this problem was deemed secondary compared to the overall goal enhanced digging ability, as an anti-counter rotation device could be retrofitted once a mechanism was selected. Different fin designs that were used

for anti-counter rotation can be seen in Appendix B. Due to the short duration of the project, the notion of designing an optimal fin design was abandoned. Two metal strips, coaxial with the motor, were attached using three metal clamping bands. The metal strips acted as the stability mechanism for a 0.64 m (24 in) long metal bar, which was placed over the strips perpendicular to the motor. During operation, the bar was steadied by hand to prevent the motor from counter rotating (Figure 4).

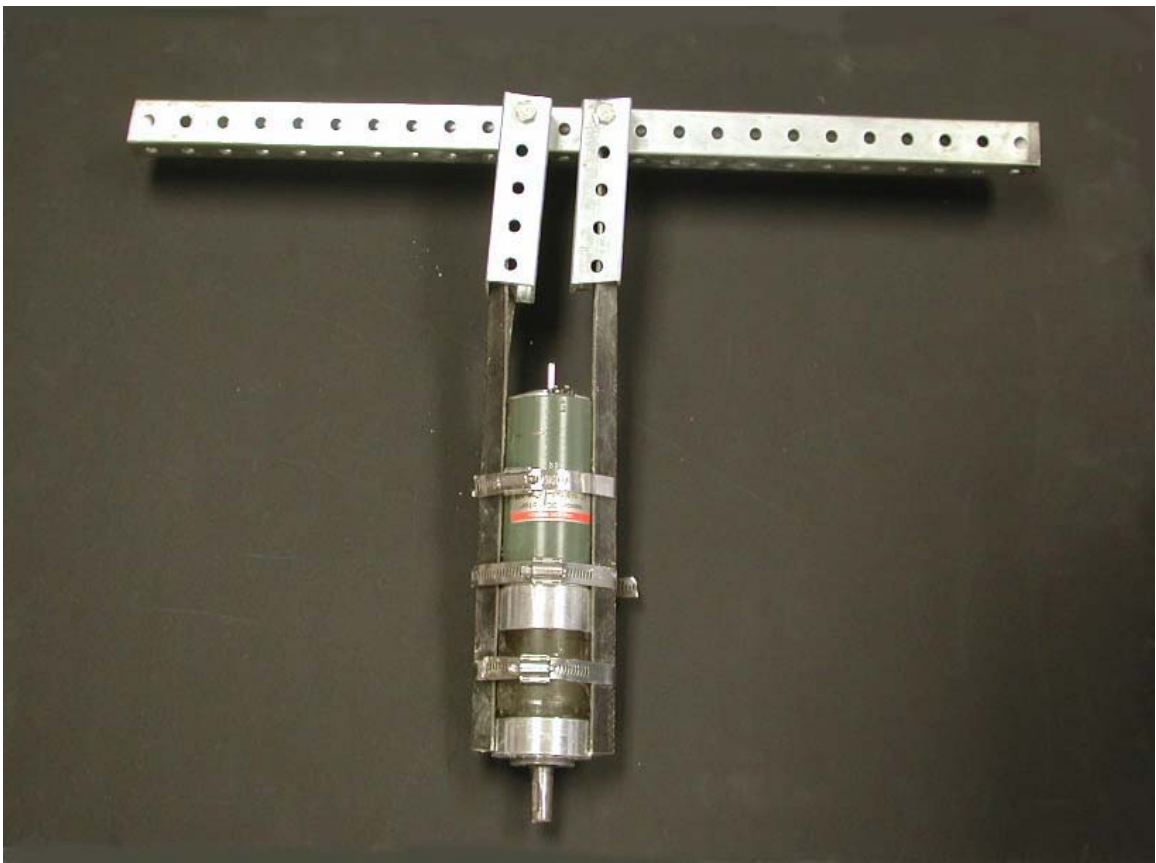


Figure 4. View of motor with attached rod for counter rotation.

4.2.3. Helical Augers

As a comparison with the conical auger, ordinary helical, gardening augers were used. These augers varied in diameter, pitch and overall length, with all tests conducted under the same conditions. Initial tests used off-the-shelf, one-piece clamp-on couplings with socket-head cap screws (Figure 5). However these were not sufficient, as the overall forces needed to turn the auger were greater than the coupling device could handle and led to the auger shaft turning within the bore hole of the coupling device.

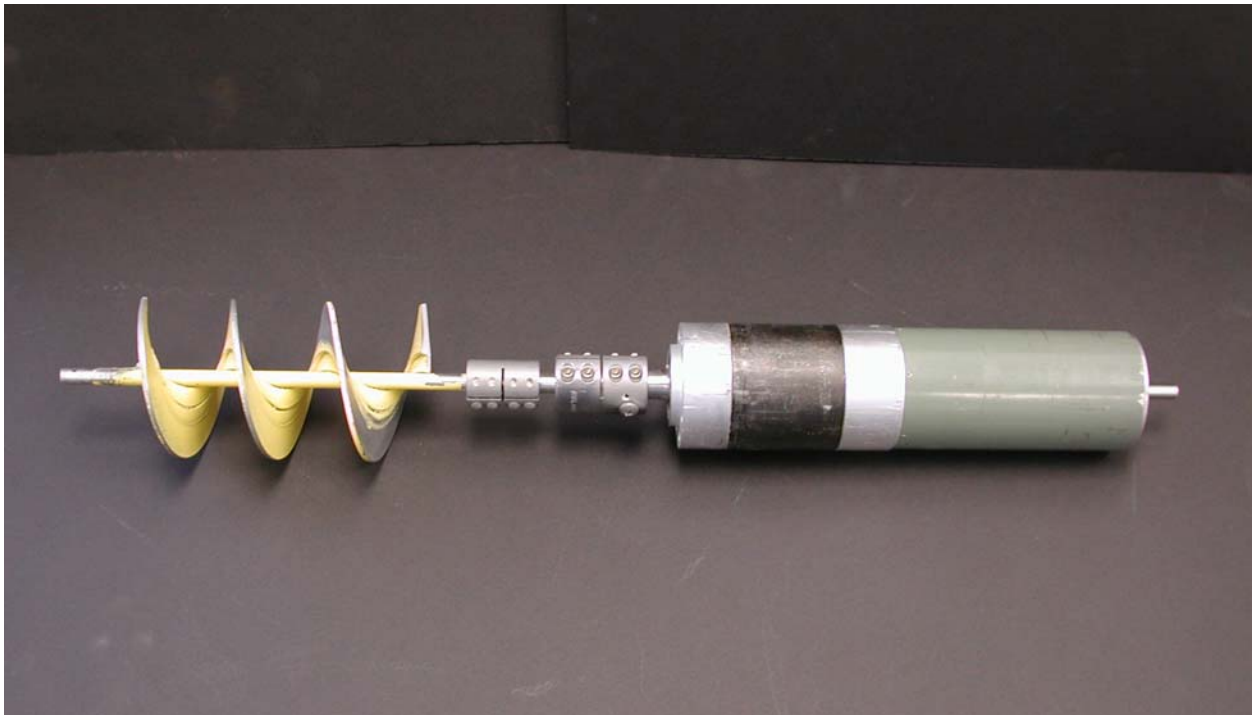


Figure 5. View of the coupling devices connecting the helical augers to the motor.

This observation led to the design of a custom attachment piece constructed from an aluminum block. The attachment piece was designed with a conical shape to help in the flow of the material from the top of the auger to the motor body. The motor and

auger were able to slide in on opposite ends, with set screws holding each in place (Figure 6). If a simple cylindrical piece, matching the diameter of the motor, was manufactured, it is believed that material flow would be hindered between the auger and motor, creating unnecessary forces that must be overcome and hence stripping of the auger in the coupling devices. A thin piece of Teflon was placed between the motor and attachment to help reduce the frictional forces between the two.

Helical augers used in the digging tests consisted of 64 mm (2.5 in) and 76 mm (3 in) diameter by 200 mm (8 in), purchased from A.M. Leonard, Inc.

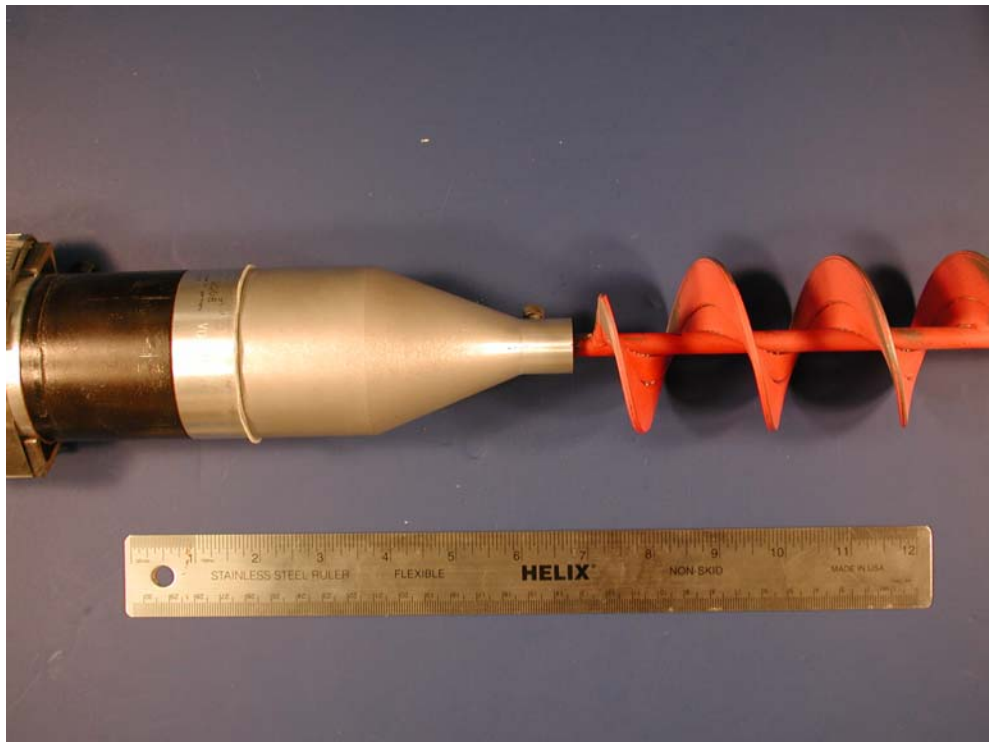


Figure 6. View of adaptor connecting the helical augers to the motor.

4.2.4. Torque Requirements

To achieve the force needed for the vehicle to dig into sand, different tests were conducted depending upon the type of forces the vehicle would encounter. Before an optimal auger could be designed, a determination of the amount of torque required for various augers to dig effectively was needed. Three groups were tested: an extremely large helical auger (200 mm, 8.0 in diameter), similar diameter conical augers (127 mm, 5.0 in and 140 mm, 5.5 in) and similar diameter helical augers (64 mm, 2.5 in and 76 mm, 3.0 in). A photograph of these five augers can be found in Figure 7.



Figure 7. View of the augers tested.

For the conical augers, a quick adaptor was installed to measure the torque required to turn the auger at different depths. The adaptor was held in place with bolts, on top of the auger, and a $\frac{3}{4}$ in nut was firmly set in the middle of the attachment. A hand-held torque wrench was coupled with the auger, with an extension placed on the nut.

4.2.5. Push Test

To gain a better understanding of the frictional forces the vehicle was likely to encounter from contact with its body (during the present project the body was generally only that of the motor) with the surrounding sand, a “push test” was needed, in which the force needed to push the body into the sand was measured. Initially, a Teflon rod ~ 51 mm (2 in) diameter, with a cone tip, was used for the tests in order to quickly estimate the force required to overcome frictional drag on a similar size vehicle body in a sand medium. The force measured increased exponentially with increasing depth. It was observed that with the same rod in identical tests, the forces experienced were not consistent from run to run, but instead increased with each run into the same sand.

It should be noted that the depth of the bucket used was only 381 mm (15 in) and the exponential increase in force could be, at least in part, a result of this factor. Also, it is believed that the increase in force with each run was due to the increase in sand compaction resulting from the previous run. With these considerations in mind, a new method of experimentation then evolved. To help eliminate the variables mentioned, a new container was employed with a depth of 610 mm (24 in), as compared with only 381 mm (15 in) for the previous setup. The diameter of the container (356 mm, 14 in) was chosen to better simulate a semi-infinite medium, in an attempt to minimize the artificial

forces on the sides of the vehicle body created by the constraint of the sand interface with the container. After each trial run, the sand was removed from the apparatus and gently “poured” back into the container, letting the sand particles randomly settle.

The test rods were comprised of five aluminum rods, each 300 mm (12 in) length, with outside diameters (OD) that ranged from 25 to 76 mm (1 to 3 in), in increments of ~13 mm (.5 in) (Figure 8).



Figure 8. Aluminum rods used for the push test.

Each rod had a conical tip, with a 75° pitch. A female thread was machined on the opposite end of the rod, for use in securing the test rod to the load cell. The latter was needed to help maintain a consistent insertion point, normal to the surface of the sand, as a major misalignment would cause a slanted insertion and would therefore have produced an increase in the force needed, skewing the results. Each test was run at a speed of 75 mm/min (~3 in/min) to a final depth of 500 mm (~20 in) with a 10 Hz data acquisition rate on a MTS tensile machine (Mechanical Testing and Simulation Inc., www.mts.com).

4.2.6. Pull Tests

An experiment was performed to determine how much force an auger can pull. Using the 64 mm (2.5 in) diameter auger, a pulley system was constructed to allow the auger to pull various weights (Figure 9). An elongated auger was added (Appendix C) to isolate the digging strength of the auger from the frictional forces exerted by the motor body. Using a similar setup as previously used for the SMA testing, two pulleys, spaced 150 mm (6 in) apart, were added to the top of the structure. Extension bars were added to the motor body (Figure 9) to allow one end of a thin wire to be attached. The wire was then pulled through the pulleys using varying weights.



Figure 9. Pull test pulley system.

4.2.7. Colored Sand Experiment

A container of layered, colored sand was used to reveal how the sand moved as a fluid body around the conical auger and motor. The set up used in this experiment can be seen in Figure 10, with five different colors layered in approximately 75 mm (~3 in) increments. Three digging experiments were run and documented using a digital video recorder.



Figure 10. Multi colored sand used to examine the auger-sand interactions.

After the initial trials, an experiment using a “sand freezing” process was conducted. The use of sodium silicate is well established in foundries for binding sand cores [64]. With the appropriate amount of sodium silicate mixed with the sand, the application of carbon dioxide (CO_2) then “freezes” the mixture at any selected moment during the digging process. The sodium silicate acts as a binder, keeping the sand mold intact without the need for any outside force. This principle was used in the colored sand experiment, freezing the sand around the conical auger and motor and then slicing it open to observe the sand-auger interaction. It was observed that the sand “freezes” well when

doubling the manufacturer's suggested 3 – 4 % by weight of sodium silicate; it was found that a mixture of 8 % by weight of sodium silicate kept the sand core stable enough to prevent crumbling when sliced into sections after CO₂ exposure. After mixing the sand with the sodium silicate manually, the colored layers were placed in the testing apparatus. The motor and conical auger were then placed in the center of the surface and allowed to dig. Upon the auger reaching bottom, or stalling, a CO₂ lance was inserted in various spots to allow the gas to diffuse throughout the sand. After hardening had occurred, a quarter piece of the sand "box" was cut out to show a profile of the sand with the auger and motor.

4.2.8. Customized Auger

As a late addition to the digging experiments, Dr. Jason Baird from the University of Missouri-Rolla, designed a custom auger specifically for digging in sand. Having acquired the necessary testing equipment, Auburn University agreed to test the design provided by Dr. Baird and his staff. Dr. Baird's auger can be seen in figure 11. A detailed AutoCAD drawing of the auger can be found in Appendix D. The design is based on a literature review that Dr. Baird modified by incorporating a reverse flight at the top of the auger to keep the material from falling inward on the borehole and to keep a continuous force on the auger bit. As the bottom flights are forcing material up, the reverse flight acts in the opposing direction to keep forcing the auger downward.

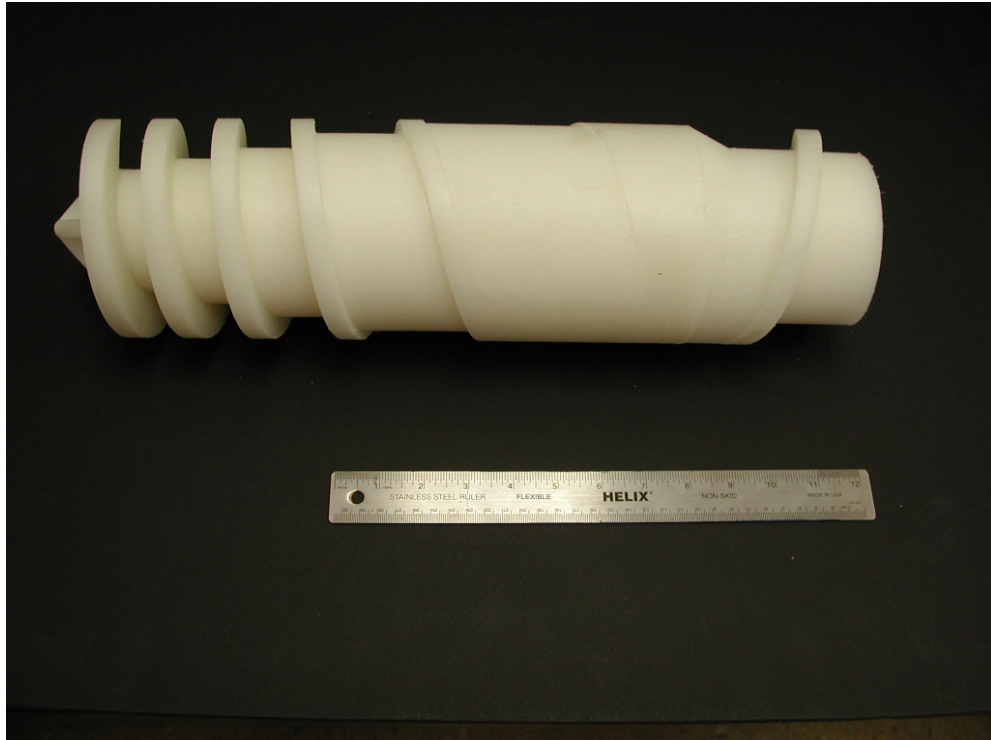


Figure 11. Digging auger designed by Dr. Baird, professor at the University of Missouri-Rolla.

4.2.8.1. Plain Sand Experiments

For comparison with the previous augers, tests were conducted in a 55-gallon drum filled with plain sand using the anti-counter rotation device shown in Figure 4. An attachment with a 100 mm diameter and 50 mm (2 in) length was constructed. Four bolts held the attachment in place with the auger, while the motor slid into a machined keyway in the center of the device.

The auger was tested using three different fixed voltages (5 V, 10 V or 15 V) with variable current. Each voltage level was repeated three times, for a total of nine trials.

The time and current at four auger depths, a quarter (130 mm, 5 in), half (230 mm, 9 in),

three-quarters (380 mm, 15 in), and final auger movement, were recorded. Before each trial, the sand was removed from the tank and reloaded in order to avoid compaction and maintain uniformity with earlier trials.

4.2.8.2. Sand Mixture Experiments

Personal communication with Dr. Baird has shown that pure sand is one of the most challenging materials to dig in, resulting in a stripping of the borehole walls, that may cause the auger to spin without descending further. It was thus decided to create a custom mixture of sand, flour and oil with a ratio of 1:1:0.2 by weight, respectively. To create this mix, off the shelf baking flour and technical grade mineral oil were mixed with the sand to fill a 114 L (30 gallon) drum with an OD of 0.41 m (16 in) and depth of 0.79 m (31 in). Mixed in small batches, the sand bed consisted of approximately 61 kg each of flour and sand, and 12 kg of mineral oil. To avoid creating a sand gradient, each new batch was mixed in with the previous layer, as opposed to simply being laid on the top. This improved the homogeneity of the mixture from top to bottom.

The auger was tested using three different fixed voltages (5 V, 10 V or 15 V) with variable current. Each voltage level was repeated three times, for a total of nine trials. The time and current at a series of auger depths of a quarter (130 mm, 5 in), half (230 mm, 9 in), three-quarters (380 mm, 15 in), and full (460 mm, 18 in), followed by multiple motor depths of a quarter (560 mm, 22 in), half (620 mm, 24 in), three-quarters (660 mm, 26 in) and final auger movement (~710 mm, 28 in), were recorded. Before each trial, the mixture was removed from the tank and reloaded, letting it settle naturally, in order to prevent compaction.

4.2.8.3. Compacted Sand Mixture Experiments

After each trial, the sand mixture was removed and then immediately reloaded into the container. However, the mixture at the bottom was inevitably compacted more than the mixture at the top due to the additional weight of the sand mixture. This was evident when the vehicle was placed on top of the sand bed, where it began to descend into the sand mixture even before the motor was started. In order to eliminate the effect of this compaction gradient, additional trials with a compacted sand bed were necessary, as the compacted bed would be more representative of a real soil and thus provide a better estimate of the required digging energy.

The auger was tested using three different fixed voltages (5 V, 10 V or 15 V) with variable current. Each voltage level was repeated three times for a total of nine trials. The time and current at multiple depths discussed previously were recorded. Before each trial, the mixture was removed from the tank and reloaded, being allowed to settle naturally. After a depth of 100-130 mm (4-5 in) had been poured in, a weight of 30 kg (66 lbs) was gently placed on the surface to compact the sand. This process was repeated until the testing container was full.

4.2.8.4. Torque Requirements of Customized Auger Experiments

A quick adaptor was installed in order to measure the torque required to turn the auger at different depths. The adaptor was held in place with bolts, on top of the auger, and a $\frac{3}{4}$ in nut was firmly set in the middle of the attachment. A hand-held torque wrench was coupled with the auger, using a ratchet extension placed on the nut.

4.2.9. Digging Energy Requirement

The digging energy (E_{dig}) was estimated based on the volume of sand displaced (Equation 1, [65]),

$$E_{dig} = \frac{V \cdot I_{max}}{A \cdot \left(\frac{d}{t}\right)} \quad (1)$$

and based on the volume of auger buried (Equation 2, [65]),

$$E_{dig} = \frac{V \cdot I_{max}}{\left(\frac{Vol_{auger}}{t}\right)} \quad (2)$$

where V is the applied voltage, I_{max} is the maximum current, A is the cross-sectional area, d is the depth, Vol_{aug} is the volume of the auger and t is the time.

4.3. Vehicle Experimentation

4.3.1. Earthworm Concept

To aid in the digging process, a model based on the way an earthworm travels was tested. Rather than simply pushing the displaced sand around the vehicle body, an attempt was made to allow the sand to move through it.

As shown in Figure 12, the motor and a 76 mm (3 in) auger were placed inside a 114 mm (~ 4.5 in) diameter tube, leaving about 89 mm (3.5 in) of the screw exposed below the tube housing to permit the auger to gain a purchase in the sand.



Figure 12. Earthworm design; Motor and 76 mm auger within a tube.

4.3.2. Friction Reduction

Another method designed to aid digging that was tested was to reduce the surface friction experienced around the motor's body. Here, air was used as the friction-reduction medium. Small diameter reinforced tubing of various lengths was placed along the body of the motor and pulses of air blow through the ends of the tubes. This caused air to blow along the surface, loosening up the sand particles and reducing the surface friction generated by the sand to motor interaction.

4.4. Biomimetic Analysis

4.4.1. Brainstorming

The primary goal of this portion of the project was to generate an analogue for implementation in a prototype vehicle designed to dig to a desired depth. The project was not expected to identify a suitable power source or provide, a global positioning system for tracking, the ability to steer, or any of the many other systems needed to create a functional vehicle. However, after piecing together off the shelf products to try to achieve this goal, it became obvious that a different approach was needed. An “outside the box” view came through the inspiration of “Mother Nature”.

Instead of trying to re-invent the wheel, the researchers chose to take a closer look at creatures that dig successfully on their own. A search of the relevant literature identified a host of creatures, including mammals, reptiles, insects and invertebrates, in numbers far too great to be useful in this study. The goal was to model something that could dig and hence a “weeding out” or selection criteria had to be stipulated.

4.4.2. First Cut

The first selection criteria used was the ability to dig to at least one body length in depth. Many creatures that do not have an underground habitat do nonetheless dig routinely. For example, dogs dig to bury or unbury things, to escape other predators or just out of apparent boredom. The fact that creatures dig is not sufficient grounds to justify an attempt to emulate their actions; therefore the ability to dig deep enough to cover one’s self completely was selected as a criterion. This criterion was fully satisfied with creatures that are characterized as “fossorial”, meaning that they live underground. Those creatures not characterized as fossorial were eliminated from this study. The

faculty and students at the University of Michigan have generated an online database of wildlife for public use, and this was used extensively to provide the central core of the project's research.

This website, animaldiversity.ummz.umich.edu, is an online encyclopedia of animals to which students at the University of Michigan contribute the most up to date information gained by researchers. By entering "fossorial" into the animal diversity's search engine, the first list of animals was selected.

4.4.3. Initial Round of Questions

The initial selection produced a list of about 50 species of animals that are fossorial. In order to avoid documenting the life history of each animal, a list of general questions (Appendix E) was used to select the pertinent details. The website only contains brief descriptions about the animals and not all the necessary information could be found elsewhere. Not all animals have been studied to the same extent, as some are observed far more intensively than others. Irrespective of whether the reason for the study is economic, academic, or maybe environmental, some animals have not been studied in enough detail to provide all the necessary information. However, by seeking to answer specific questions for each, the differences between the animals became more apparent and more focused questions could be included in the next round.

4.4.4. Second Round of Questions

After learning more about the differences between the animals, a second list of questions was used to gain specific knowledge. These questions generally examined issues related to the metrics used to describe the animals, which were divided into three main categories: general characteristics, digging mechanism and bioefficiency.

The general characteristics described the appearance and the social aspects of the creatures. The second category, digging mechanism, comprised four subcategories: performance, namely the depth and rate of the digging; mechanical, or details of the digging apparatus of the creature, such as motion and efficiency; chemical, as some creatures have chemical capabilities to aid in their digging process; and environmental, to examine the conditions and the materials they dig in. The third and final category is bioefficiency, which considers the availability and calorific value of the food sources ingested and how they give the individual creatures the energy they need to dig.

4.4.5. Weighting System

Not all this information was readily available, however this did provide a way to separate the creatures from one another, and compare the best candidate versus the worst candidate. After reviewing the possible metrics, a new categorization was established, that focused on the information that would be important for replicating the creature: speed, depth, power, material substance, mechanical complexity, geographic range, and the size of the body of the creature. This new set of categories was used to create a weighting system that could be used to assign a numerical value for each creature.

Each category had its own weighted percentage and set of related metrics. Each metric was rated on a scale of one to five, based on the information known. However important the metric might be, not all of the information was available. The lack of information could not be used to justify rating a metric as unnecessary, as this metric might still be vital. For this reason, two calculation methodologies were considered, both with and without an allowance for unknown information. Each metric had two values: a raw score using arbitrary values (*e.g.* 3 out of 5) for the unknowns, and a raw score

implementing only the known values. For organisms with little available data, the use of an arbitrary value for unknown categories tended to push the score towards an “average” score, whereas ignoring the categories without data tended to overweight the importance of the available data. Using both methods did not correct for this shortcoming, but it did help in interpreting the meaning of the scores.

After all the metrics had been assigned an appropriate score, the raw scores were weighted and added together for a final score. Each creature had two final scores; with and without the arbitrary values for the unknown. Because the digging vehicle would be used in many different situations, each creature was evaluated for three desired scenarios: Scenario 1, small body (≤ 300 mm; 12 in) at low depths (≤ 1.52 m; 60 in); scenario 2, small body (≤ 300 mm; 12 in) at medium depths (1.52 m; 60 in – 6.10 m; 240 in) and scenario 3, medium body (300 mm; 12 in – 910 mm; 36 in) at deep depths (≥ 6.10 m; 240 in). Thus, each creature had six final scores, two for each scenario (Appendix F).

4.4.6. Flow Chart for Biomimetic Design

After the creature has been chosen based on the final scores, an overall look was needed for design purposes. A flow chart was created to aid in this process. The flow chart was designed to identify the power requirements, materials and any special features that need to be incorporated into the final vehicle and the overall cost effectiveness of the vehicle. After all these aspects have been covered, if it was found that the chosen creature was not cost effective, a redesign would be necessary in order to select cheaper materials, an alternative power source or possibly a different creature that would be more suitable overall. This process can be seen in Appendix G.

5. EXPERIMENTAL RESULTS

5.1. SMA Testing Results

5.1.1. First Batch

The springs were elongated to their maximum length (without resulting in irreversible damage) of about 305 mm (12 in). While applying a constant current and load, the actuation distance was measured manually, hence human error, (approximately +/- 1 mm), may account for a portion of the variability observed between tests of similar current and load. Table 1 shows the observations for springs at different loads and currents. It should be noted that all tests were performed in constant current mode and the voltage was allowed to fluctuate. This is important since a change in resistivity is observed when the wire undergoes its phase transformation. The voltages noted are the averages seen after a drop, due to the lower resistance once actuation has occurred.

The average electromagnetic actuation efficiency of the SMAs was calculated using the following expression [20]:

$$\text{Eff}_{\text{av}} = \frac{\text{Force}(N) \times \text{Stroke}(m)}{\text{volts} \times \text{amps} \times \text{time}(\text{sec})} \quad (3)$$

which corresponds to the mechanical work divided by the electrical energy supplied.

Table 1. SMA conversion efficiency of the first batch of springs

Force		Other Parameters				
Lbs	N	Stroke (m)	EMF (V)	Current (A)	Time (s)	% Efficiency
0.02	0.07	0.17	2.5	3	49	0.003
1	4	0.13	2.5	3	59	0.13
2	9	0.07	2.5	3	75	0.11
3	13	0.01	2.5	3	87	0.03
4	18	0	2.5	3		
5	22	0	2.5	3		
Force		Other Parameters				
Lbs	N	Stroke (m)	EMF (V)	Current (A)	Time (s)	% Efficiency
0.02	0.07	0.16	3.3	4	25	0.003
1	4	0.13	3.3	4	30	0.15
2	9	0.11	3.3	4	39	0.19
3	13	0.08	3.3	4	45	0.17
4	18	0.05	3.3	4	67	0.10
5	22	0.01	3.3	4	94	0.02
Force		Other Parameters				
Lbs	N	Stroke (m)	EMF (V)	Current (A)	Time (s)	% Efficiency
0.02	0.07	0.15	3.7	5	19	0.003
1	4	0.13	3.7	5	25	0.12
2	9	0.10	3.7	5	30	0.17
3	13	0.08	3.7	5	42	0.14
4	18	0.05	3.7	5	42	0.12
5	22	0.03	3.7	5	70	0.05
Force		Other Parameters				
Lbs	N	Stroke (m)	EMF (V)	Current (A)	Time (s)	% Efficiency
0.02	0.07	0.16	4.7	6	12	0.003
1	4	0.14	4.7	6	15	0.14
2	9	0.11	4.7	6	20	0.17
3	13	0.09	4.7	6	31	0.14
4	18	0.07	4.7	6	39	0.11
5	22	0.04	4.7	6	44	0.08

To better visualize the capability of the SMAs, a graph of current vs. stroke was generated from these results. Figure 13 represents the average maximum SMA spring contraction distance (i.e. stroke) obtained when lifting various weights (0-22 N in 4 N increments, 0-5 lbs in 1 lb increments) versus a range of input currents (3-6 A in 1 A increments). Three amperes was the minimum current tested due to the fact that anything less provided insufficient heating of the SMA spring. Six amperes was the maximum current tested since this was the largest integer value that the power supply employed at that time was capable of producing. The graph shows that large strokes can be obtained at low or no loads with minimal energy input (e.g. 3 A at 2.5 V = 7.5 W). However, at greater loads (i.e. 13-22 N, 3-5 lbs) more energy input is necessary (e.g. 5 A at 3.7 V = 18.5 W). In addition, considerably smaller strokes were achieved at greater loads. This is understandable, considering that SMAs can produce either large strokes or large forces, but not both simultaneously. Note that the error bars included in the graph show the variability in the strokes obtained. This variability is attributed to both multiple individuals performing the tests and intrinsic variability from spring to spring.

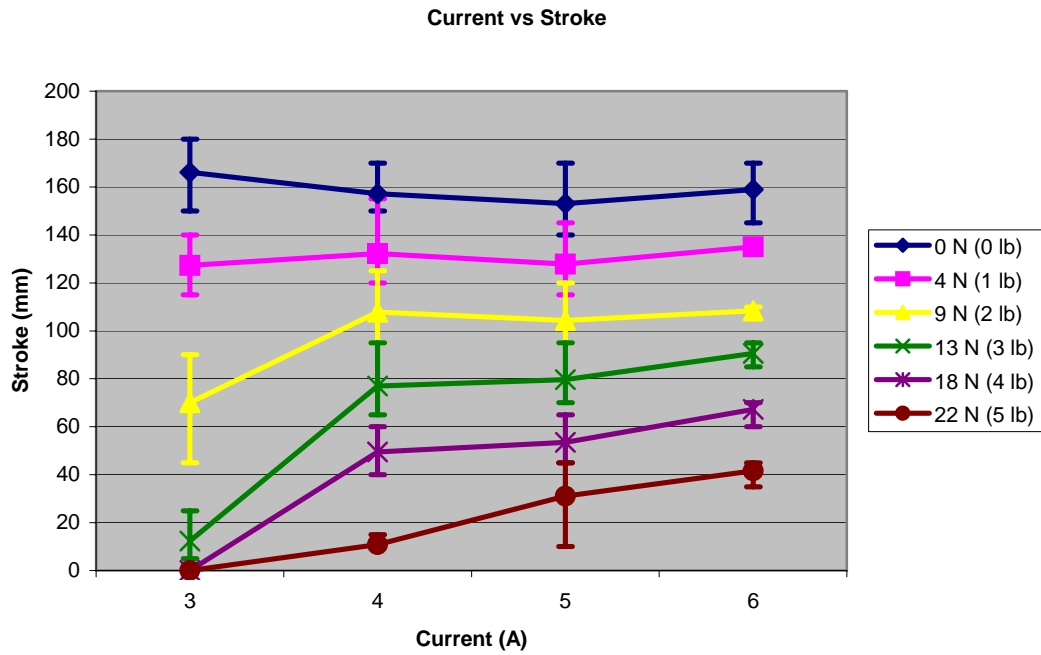


Figure 13. Graphical representation of the current vs. stroke results with error bars showing the standard deviation.

Figure 14 represents the average time needed to actuate when subjected to various currents versus the same amount of weight. It should be noted that at 3 A and above a force of 13 N, the time required for actuation is much greater when compared to those at higher currents.

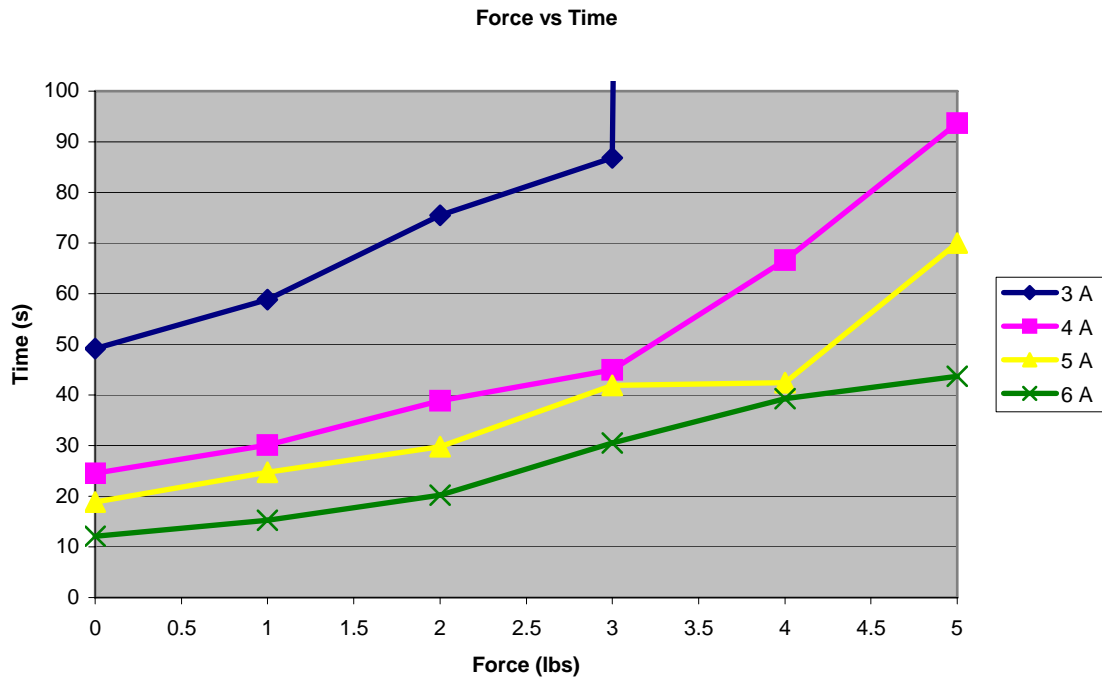


Figure 14. Graphical representation of force vs. time results (note at 3 A lifting of a 3 N load did not occur so the time is not shown).

5.1.2. Second Batch

It was assumed that the larger springs would be able to handle larger loads along with a larger current, so testing was to start at a 45 N (10 lbs) load at 10 A, increase in increments of 9 N (2 lbs) and 2 A up to 89 N (20 lbs) and 20 A with a 300 second (5 minute) cooling period in between each run. Three springs were tested, however, the actuation distances were not repeatable. Individual spring results are in Appendix H. During one run, after about 20 s at 20 A, deformation of the spring occurred as the current was being applied. The spring literally started to uncoil and stretch with the weight still attached. The attainable actuation distance dropped from 170 mm (initial test) to 90 mm (after deformation). This same abnormality was observed even at lower currents and loads. Table 2 shows the results from a spring at these lower conditions.

The actuation distances in the second round of testing at the same (low) currents were reduced when compared to the initial distances. These observations are the same as seen in previous experiments; however, the differences were not as extreme as previous recordings. Thus it might be that the lower currents were still harmful but took longer to cause extreme damage.

Table 2a. Initial observations of a SMA spring at low currents and loads.

Force		Other Parameters				
Lbs	N	Stroke (m)	EMF (V)	Current (A)	Time (s)	% Efficiency
6	27	0.19	3.2	9	34	0.52
6	27	0.19	3.2	9	32	0.56
6	27	0.18	3.2	9	33	0.51
6	27	0.17	2.9	8	43	0.46
6	27	0.17	2.9	8	44	0.45
6	27	0.17	2.9	8	43	0.46
6	27	0.17	2.5	7	107	0.25
6	27	0.16	2.5	7	109	0.23
6	27	0.16	2.5	7	107	0.23

2b. Results of SMA spring at low currents and loads; second testing unable to achieve initial results.

Force		Other Parameters				
Lbs	N	Stroke (m)	EMF (V)	Current (A)	Time (s)	% Efficiency
6	27	0.17	3.2	9	36	0.44
6	27	0.17	3.2	9	35	0.46
6	27	0.17	3.2	9	33	0.48
6	27	0.16	2.9	8	44	0.42
6	27	0.16	2.9	8	45	0.41
6	27	0.16	2.9	8	44	0.42
6	27	0.17	2.5	7	106	0.25
6	27	0.16	2.5	7	105	0.24
6	27	0.15	2.5	7	107	0.22

The next point of interest was the SMA actuation efficiency, expressed in terms of converting electric power to useful work. It was found that the range of efficiency was very low for the first batch, with the efficiency ranging from as low as .003% to as high

as 0.18%, depending on the amount of weight and/or current (Table 1). An average energy conversion efficiency for a “typical” NiTi SMA is only about 5%, as most of the energy is dissipated in heating the wire before the transformation begins, especially given the high heat loss from the large surface area of a coiled spring. Nonetheless, the results were still far below the “accepted” efficiency of Nitinol SMAs. One possible explanation of the low efficiency was that the heating cycled employed for the work was not optimized for the wires used. It was theorized by the project team that higher currents, such as 9-10 A, should decrease the amount of time needed for the wire to go through transformation. An optimum compromise between the two variables was needed.

In contrast to the small energy conversion efficiency, the wire had a very high lifting capability to spring weight ratio. With a total weight of 7 g, the SMA wire can lift 22 N, giving it a 3 N per gram (~ 3.0 lbs/oz) ratio.

It was noted that the efficiency of the second half of the SMA order had greatly increased over that of the first half. In the case of spring 1, the overall average of the efficiency was 0.5 % — three and half times that of the first batch efficiency estimate of 0.14 %. In the case of spring 2, the efficiency dropped from 0.5 % to 0.4 %. In the case of spring 3, initial testing showed an average of 0.46 % and a drop to 0.41 % for the second testing.

5.2. Auger Testing

5.2.1. Torque Requirements

Figure 15 shows the amount of torque needed to dig as the depth increases. All three groups of augers required increased torque with depth, although some experienced this increase at a higher rate than others. Using a hand held torque wrench, the data may be somewhat variable due to human error (approximately +/- 5 Nm). Overall, it was observed that the torque requirements needed to turn the large 200 mm (8 in) auger were more than that was physically possible for the experimenters below 305 mm (12 in) of sand. Conical augers of similar diameter experienced a steady increase in torque throughout the testing, but stopped at ~ 610 mm (24 in) due to equipment limitations (*i.e.* exceeded the range of the torque wrench). The smaller diameter set of similar helical augers experienced the least amount of torque needed when compared at the final depth of 610 mm (24 in).

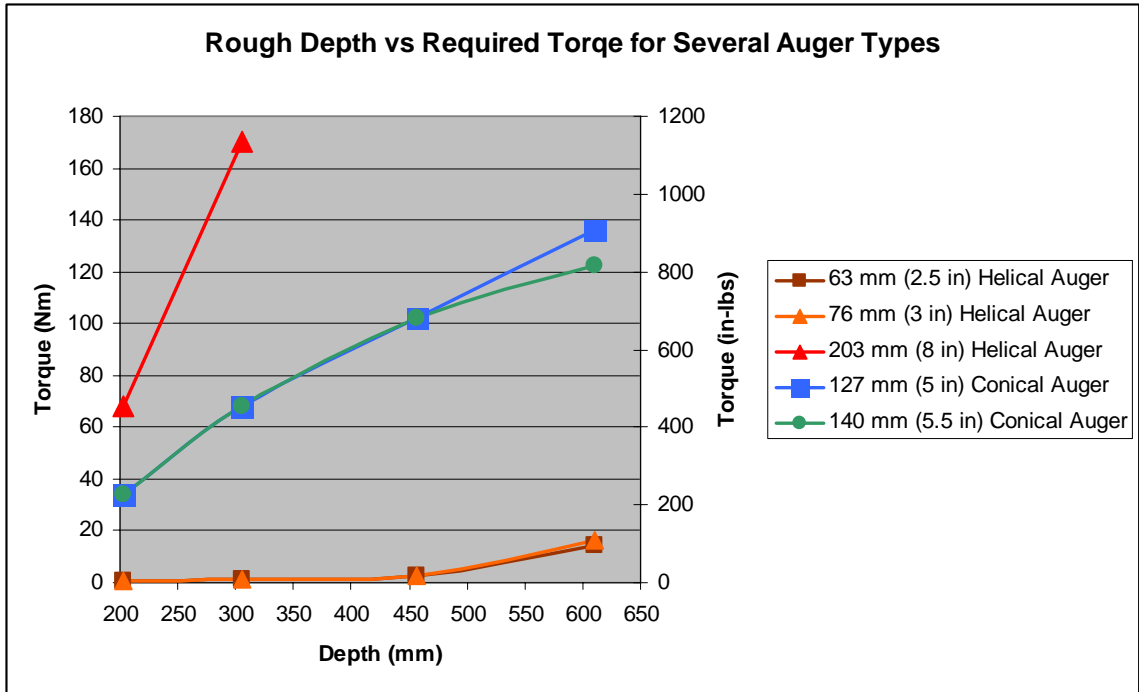


Figure 15. Depth vs Torque for various auger diameters.

5.2.2. Push Test

The results were generally as expected, with the required force greatly increasing with increasing rod diameter (Figure 16). As the depth increased, so did the amount of force needed to compensate for the increasing contact area with the sand and, hence, to overcome the frictional forces on the rod. At about 300 mm (12 in) depth, the rod was fully inserted and the entire rod surface area was in contact with the surrounding sand, yet there was still a significant increase in the amount of force needed to continue to push in the larger diameter bars. Some of this could be explained by the use of a push rod which attached the push test sample to the screw driven testing machine (Mechanical Testing and Simulation Inc., www.mts.com), but the diameter of this push rod was only ~25 mm (1 in) and so this should have been relatively insignificant when pushing the ~51 mm (~ 2

in) and larger OD samples. The observation that the required insertion force increased with depth beyond the sample length for the large diameter rods (50 mm, 2 in and greater diameter), but leveled off somewhat for smaller diameter rods, has yet to be explained.

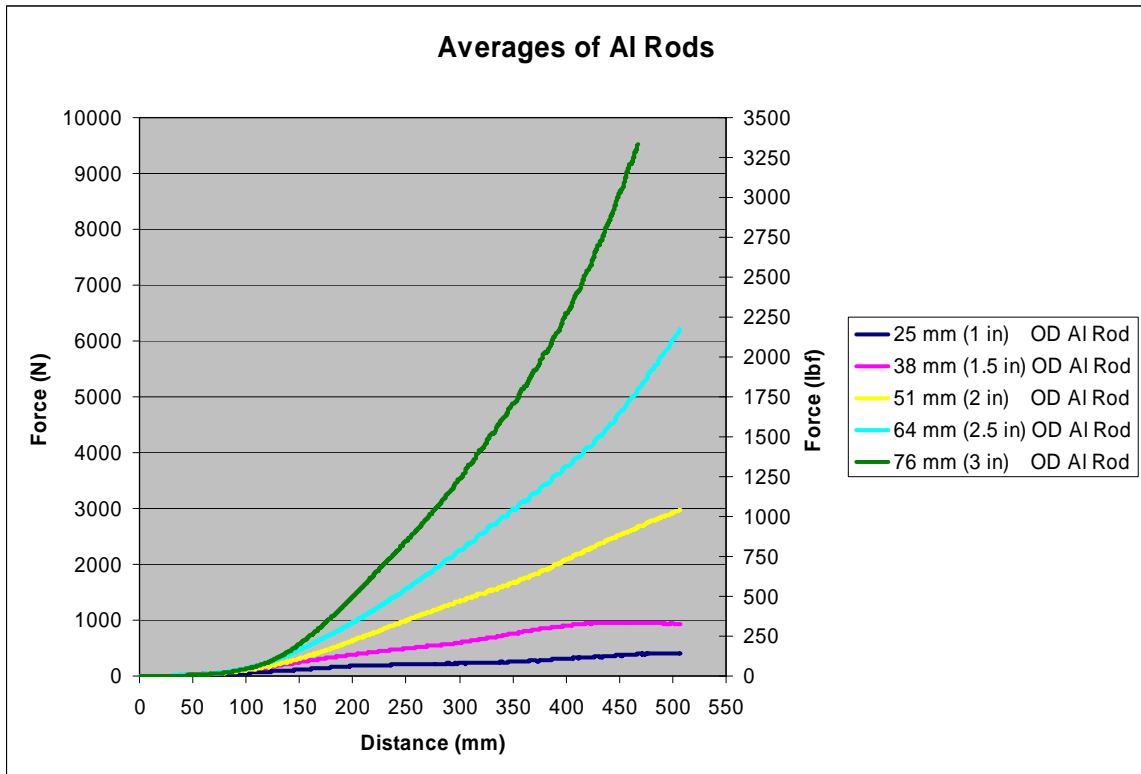


Figure 16. The average forces needed to push the different OD aluminum rods into a sand medium at 75 mm/min (3 in/min).

5.2.3. Pull Test

Using the 64 mm (2.5 in) diameter auger, it was found that the auger with the motor, which weighed 46 N (10.5 lbs), could only pull a load of 55 N (12.3 lbs) before it stopped digging. With the auger ~ 250 mm (10 in) into the sand, weight was added and the motor was observed to see if any further descent occurred.

With the addition of 4 N (1 lb) to the 55 N, the auger ceased to bite and just spun in the sand. Subtracting the weight of the motor from the weight pulled, the total force was about 8 N.

The experiment was repeated with the ~ 75 mm (3 in) auger, however an elongated auger was not available at the time and so testing proceeded with the normal set up as shown previously in figure 6. The results showed a considerably different behavior, however; with weights up to 46 N (10.5 lbs) the auger was able to dig to about 480 mm (19 in) deep, which is the length of the auger and motor body combined. Not only was the auger pulling the weight, but it was also overcoming the frictional forces encountered due to the surface of the motor. The only hypothesis to explain this observation was that since the auger had been severely roughened from the previous digging trials in the sand it was able to bite the sand in a more effective manner. The increase in diameter might also have aided in the digging, giving the auger more surface area to interact with the sand.

5.2.4. Colored Sand Experiment

The profile seen in Figure 17 showed little sand mixing, as the layers were still largely intact around the auger. Teeth marks from the auger can also be seen from the downward motion. The dip in the colors in each layer that is visible to the right of the auger was artificially created and should be excluded from any observations. This was due to the insertion of the lance used to add the carbon dioxide.

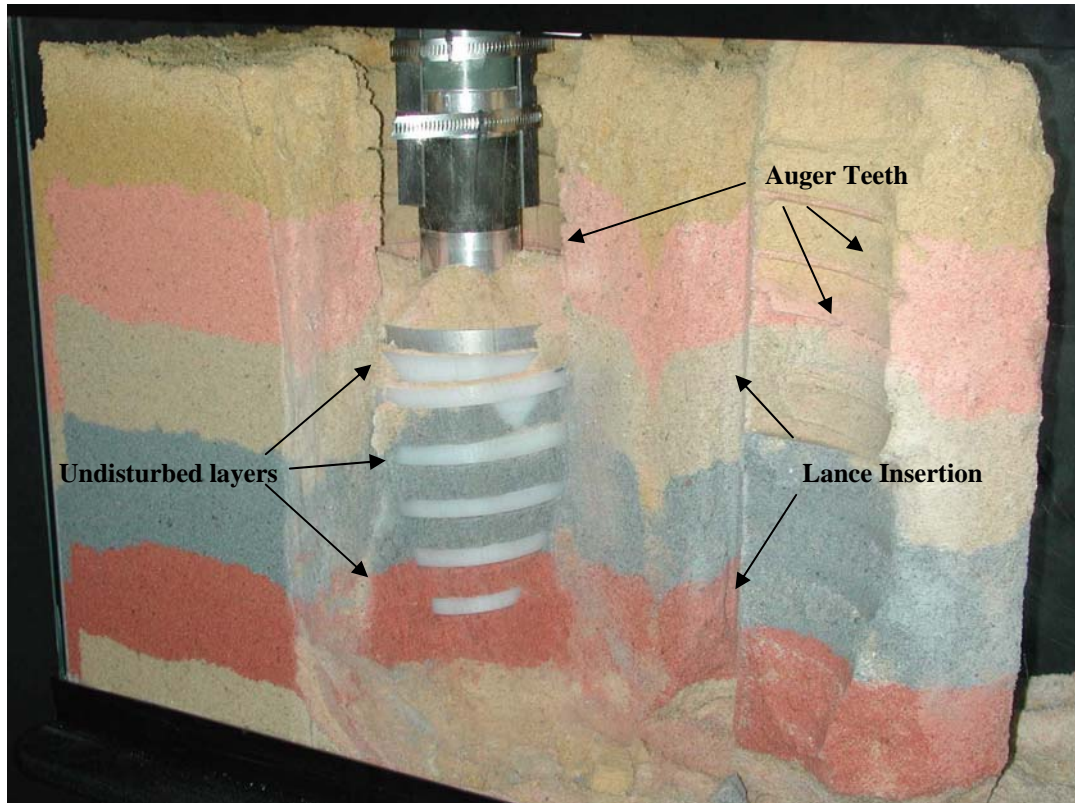


Figure 17. Profile of digging trial using a sand core.

Observations made with the frozen sand confirmed that sand was not carried up to the surface. This indicates the auger was pushing the displaced sand outward, rather than carrying it upward, as an auger should. Indeed, the walls of the sand tank were observed to bulge outwards during digging, as would be expected if sand was displaced outwards, rather than upwards. This would seem, at least in part, to explain the large torque needed for digging. An additional observation was that the tip of the auger appeared to have churned up the sand, rather than gripping it, in a fashion reminiscent of a screw that has stripped its hole. Thus, the auger employed for the test appeared to have lost its grip on the sand. This would account for the observation that the digging tended to stall, before the torque capabilities of the motor were exceeded.

5.3. Customized Auger

5.3.1. Plain Sand

The results, average time, average current, standard deviation (STDEV) for time and current and estimated digging energy are summarized in Table 3a and 3b. As in previous experiments, the digging energy has been calculated based on both the volume of sand displaced and the depth to which the auger is buried (see 4.2.9 Digging Energy Requirement, Equation 1 & 2)

Table 3a. Digging results using fixed voltages of 5, 10 and 15 V. Average values for three trials.

		Begin Digging	Auger Quarter Buried	Auger Half Buried	Auger Three-Quarters Buried	Final
5 V	Average Time (s)	0	61	160	410	440
	STDEV (Time)	0.0	11	14	27	5.0
	Average Amperes (A)	0.6	1.1	2.0	5.4	6.2
	STDEV (Amperes)	0.0	0.02	0.10	0.3	0.01
10 V	Average Time (s)	0	31	71	145	170
	STDEV (Time)	0.0	3.1	3.2	6.0	3.0
	Average Amperes (A)	0.6	1.1	1.6	4.6	6.2
	STDEV (Amperes)	0.0	0.01	0.4	0.5	0.01
15 V	Average Time (s)	0	20	47	89	110
	STDEV (Time)	0.0	1.0	3.2	5.5	2.5
	Average Amperes (A)	0.6	1.1	2.0	4.3	6.2
	STDEV (Amperes)	0.02	0.05	0.05	0.4	0.0

Table 3b. Estimated digging energy using fixed voltages of 5, 10 and 15 V.

	5 V	10 V	15 V
Estimated Digging Energy (per m ³ of sand displaced)	4.2 MJ	3.2 MJ	2.5 MJ
Estimated Digging Energy (per m ³ of auger buried)	3.8 MJ	2.9 MJ	2.8 MJ

5.3.2. Sand Mixture

The results, average time, average current, standard deviation (STDEV) for time and current and estimated digging energy are summarized in Table 4a and 4b. As in previous experiments, the digging energy has been calculated based on both the volume of sand displaced and depth to which the auger is buried (see 4.2.9 Digging Energy Requirement, Equation 1 & 2)

Table 4a. Digging results using fixed voltages of 5, 10 and 15 V. Average values for three trials.

		Begin Digging	Auger Quarter Buried	Auger Half Buried	Auger Three-Quarters Buried	Auger Fully Buried	Motor Quarter Buried	Motor Half Buried	Motor Three-Quarter Buried	Final
5 V	Average Time (s)	0	36	98	163	240	340	410	320	500
	STDEV (Time)	0.0	9.5	4.5	1.00	1.5	18	43	275	45
	Average Amperes (A)	0.5	0.8	1.2	1.7	2.1	2.6	3.1	2.1	3.1
	STDEV (Amperes)	0.0	0.07	0.03	0.11	0.16	0.23	0.36	1.9	0.43
10 V	Average Time (s)	0	10	35	60	85	115	135	160	187
	STDEV (Time)	0.0	2.1	1.00	1.00	3.5	3.00	3.6	12	12
	Average Amperes (A)	0.6	0.8	1.0	1.4	1.8	2.3	2.7	3.1	3.2
	STDEV (Amperes)	0.02	0.05	0.03	0.03	0.03	0.06	0.19	0.14	0.67
15 V	Average Time (s)	0	9	24	40	58	75	86	106	118
	STDEV (Time)	0.0	1.5	1.5	1.7	2.1	2.9	4.00	3.8	3.0
	Average Amperes (A)	0.6	0.8	1.1	1.6	1.9	2.3	2.6	3.1	2.7
	STDEV (Amperes)	0.02	0.06	0.08	0.02	0.09	0.05	0.20	0.13	0.12

Table 4b. Estimated digging energy using fixed voltages of 5, 10 and 15 V.

	5 V	10 V	15 V
Estimated Digging Energy (per m ³ of sand displaced)	1.7 MJ	1.3 MJ	.98 MJ
Estimated Digging Energy (per m ³ of auger buried)	2.8 MJ	2.1 MJ	1.3 MJ

5.3.3. Compacted Sand Mixture

The results, average time, average current, standard deviation (STDEV) for time and current and estimated digging energy are summarized in Table 5a and 5b. As in previous experiments, the digging energy has been calculated based on both the volume of sand displaced and the depth to which the auger is buried (see 4.2.9 Digging Energy Requirement, Equation 1 & 2)

Table 5a. Digging results using fixed voltages of 5, 10 and 15 V. Average values for three trials.

		Begin Digging	Auger Quarter Buried	Auger Half Buried	Auger Three-Quarters Buried	Auger Fully Buried	Motor Quarter Buried	Motor Half Buried	Motor Three-Quarter Buried	Final
5 V	Average Time (s)	0	62	147	232	350	N/A	N/A	N/A	447
	STDEV (Time)	0.0	6.5	19.6	24.1	19.4	N/A	N/A	N/A	6.5
	Average Amperes (A)	0.5	0.8	1.2	1.9	2.5	N/A	N/A	N/A	3.4
	STDEV (Amperes)	0.02	0.06	0.06	0.10	0.09	N/A	N/A	N/A	0.03
10 V	Average Time (s)	0	29	65	99	133	169	190	N/A	196
	STDEV (Time)	0.0	3.0	3.0	3.6	3.6	6.1	6.7	N/A	2.5
	Average Amperes (A)	0.5	0.9	1.2	1.9	2.3	2.9	3.2	N/A	3.3
	STDEV (Amperes)	0.10	0.04	0.07	0.04	0.08	0.22	0.14	N/A	0.06
15 V	Average Time (s)	0	16	42	64	88	108	121	130	130
	STDEV (Time)	0.0	3.0	7.5	9.5	9.7	11.4	10.8	12.3	12.0
	Average Amperes (A)	0.5	0.8	1.2	1.8	2.3	2.7	2.9	3.3	3.0
	STDEV (Amperes)	0.04	0.06	0.07	0.08	0.03	0.05	0.16	0.05	0.1

Table 5b. Estimated digging energy using fixed voltages of 5, 10 and 15 V.

	5 V	10 V	15 V
Estimated Digging Energy (per m ³ of sand displaced)	1.7 MJ/m ³	1.3 MJ/m ³	1.3 MJ/m ³
Estimated Digging Energy (per m ³ of auger buried)	2.0 MJ/m ³	1.9 MJ/m ³	2.0 MJ/m ³

5.3.4. Torque Requirement for Customized Auger Experiments

In a plain sand bed, with a high friction stress, the custom auger observed a torque requirement of 135 Nm, once fully buried. With the addition of the flour and oil, the torque was reduced to only 27 Nm. However, with a compacted bed consisting of sand, flour and oil, the torque increased to 81 Nm. The results can be found in Table 6.

Table 6. The torque requirements, measured in Newton-meters, for the custom auger testing.

	Plain Sand	Sand Mixture	Compacted Sand Mixture
Measured Torque (Nm)	135 (1200 in-lbs)	27 (240 in-lbs)	81 (720 in-lbs)

5.4. Vehicle Experimentation

5.4.1. Earthworm Concept

The motor had no problem burying the auger during the initial run, but ceased its downward movement once the sand level reached the motor itself. The voltage was kept at a constant 15 V. The current however, started at 0.6 A but quickly jumped to about 2 A, as the sand level reached the motor (Figure 18). Due to the higher torque needed, the attachment started to slip around the auger extension instead of rotating the

auger. The conical adapter was then machined to overcome this problem. Unfortunately, due to the limited time and funding available, there was no opportunity to conduct a retest.



Figure 18. Stopping point of the earthworm design.

5.4.2. Friction Reduction

Tube placement was tested at the nose of the cone attachment, the beginning of the motor body and the middle of the motor body. Placing the tube ends at the nose of the cone/top of the auger proved unreliable, as the moving part (adapter) caused interference. The rotation of the cone caused the tubes to become horizontal in the sand, thus rendering them useless. Placement in the middle of the body of the motor did not allow full involvement of the air.

The device was unable to dig far enough down for the tubes to be effective with the air pressure and the device stopped well before the tubes were below the surface of the sand. These issues led to the decision to keep the tubes level with the beginning of the motor (Figure 19).



Figure 19. Visual of motor with air hoses to help reduce the surface friction.

However, testing at this position was also found to be unsuccessful. With air blowing straight down into the sand, it was thought that there was insufficient air to surface interaction to be really effective. Therefore, small holes were placed at ~ 25 mm, (1 in) intervals along the length of the tube, parallel to the surface of the motor.

With various pulse intervals, the digger produced the same result; a depth of about 380 mm (15 in). This suggests that either the frictional forces were not as big a problem as the inability of the auger to dig consistently, or that a more sophisticated air delivery system is required.

5.5. Biomimetic Results

5.5.1. Weighted Results

A weighting system was created to assign each item of information a corresponding value. A scale of 1 – 5 denoted each piece of information as being useful to the model (5) or being a hindrance to efficient digging (1). Seven primary metrics were created, with four of the seven based on the total value of the information (speed, power, material substance, mechanical complexity) and three of the seven based on the appropriateness of the information to a digging scenario (depth, geographic range, size of body). For example, the razor clam can dig in a timely manner for its body size and can be given a direct value based on the speed attained. However, because of its small size and nature of its environment (water), these are not appropriate conditions when trying to build a large-size digging vehicle for surface applications. Therefore, it would receive a high mark for its speed but low marks for the appropriateness of its size and geographic range. If, however, the scenario were to build a water-based digger, then the razor clam would receive high marks for the appropriate geographic range. As mentioned in section 1.4.5 Weighting System, each scenario has two scores, with and without arbitrary values. The following creatures were identified as worth additional study based on the output from the weighting system. Scenario 1 with arbitrary values produced tied scores between the brown rat, narrow faced kangaroo rat and the golden mantled ground

squirrel. The great gerbil was rated the most useful for scenario 2 with arbitrary values. The Townsend mole had the best score for scenarios 1 and 2 without arbitrary values. The termite is deemed the best candidate for both cases of scenario 3. Results from all the creatures researched can be found in Appendix I.

It should be noted that none of the information was given a mandatory requirement for the scenarios; this is why the termite came out with the highest score for scenario 3, deep depths and medium sized body. The termite was given a low mark for its body size however a high mark for its deep depths. This anomaly is based on the amount of information that was found for each creature. Creatures that fit the classification of medium sized body could not dig as deep or did not have enough information to warrant a high enough score. The mole however was of appropriate size and is better suited for shallow to medium depths, hence receiving a higher score without using arbitrary values. All the resulting information for each creature can be found in Appendix J.

6. DISCUSSION

6.1. SMA Testing Procedure

During testing of the SMAs, many things may have been responsible for variations in the experimental procedure that could skew the results. First, the testing was performed with the help of several students; the testing was not performed by the same one or two people throughout the life of the project. This may have led to some variation in the readings, for example, how the yard stick was read. Also, there was considerable room for error in the recording of the time at the end point of the experiment. Sufficient time was required to satisfy the observer that all movement of the SMA had ceased and no more lifting was going to be accomplished. While assessing this, some observers may have allowed more time than was necessary to complete the experiment. On many occasions, the spring stopped prematurely due to uneven heating of the wire. Once an even distribution of heat had been achieved, the coil would then continue to lift the weight. Because of this phenomenon, it is reasonable to assume that different observers would allow different amounts of time to ensure the endpoint had been reached. Another example was the fact that all the springs were tested at the same stretched length. For the smaller springs in the first batch, initial testing at various stretched lengths was not performed to determine the optimum working length. If the first batch was overstretched, this could have decreased the SMA's power. The larger springs in the second batch, were tested at the same length as the first batch,

although as though they were bigger, they could have theoretically handled a greater lifting distance. By failing to normalize the distance, the second batch could have appeared to have a higher efficiency than was actually justified by the results.

6.2. Auger Testing

6.2.1. Conical Auger

The conical auger was designed based on a “back of the envelope” idea, although after viewing the final product, the research team agreed that this was not in fact the best approach. The design produced was un-symmetrical and no preliminary study of the literature was conducted to support the shape. Two augers were fabricated, one using a high density polymer and the other bare aluminum. However, problems were encountered as the aluminum was too heavy for the motor to handle. The polymer auger was hard enough to withstand erosion to some extent but it was still affected by the sand, leaving many abrasions that were visible to by the naked eye and could be felt by hand. The main problem however was the design itself, which required high torques. This was attributed to the wide base and the thick flights spiraling around the center. These produced large surface areas that contributed to the large frictional forces experienced. Also, due to its design, the auger would sometimes strip the sand in the borehole, hence preventing any further descent. A visual inspection during the experiments revealed that the auger often pushed the sand outward instead of upward and the auger would simply spin in place. Another problem that had to be addressed was that large torques were required during the experiments that were too severe for simple anti-counter rotation devices to deal with, so a hand held stabilizing mechanism was needed. The deeper the vehicle penetrated, the larger the force needed to stabilize the motor and this became a

considerable strain on the operator. Eventually the strain on the motor would become too great, leading to stalling out, in the event that the auger did not strip the borehole.

6.2.2. Helical Augers

Industrial helical augers were purchased off the shelf. The decision to test commercially available models to replace the conical auger initially used was dictated by their proven track record for post hole digging in real world situations. However, in industrial applications, they are equipped with an ample power supply capable of applying sufficient force, weight on bit, and torque, to overcome frictional forces, to push the auger down into the earth. For this experiment, the small diameter (64 mm, 2.5 in and 76 mm, 3.0 in) helical augers required a much lower torque to spin through sand compared to the conical augers. This can be attributed to the smaller volume of each helical auger. The helical augers have thin flights and a smaller core diameter which greatly reduces the surface area. However, abrasive markings were still visible evidenced by large areas of paint that had been eroded away to expose the base metal. In contrast, the large diameter helical auger (200 mm, 8.0 in) had an extremely high torque value due to its larger flights producing a larger surface area and moving a larger amount of sand. Both the small diameter helical augers were difficult to use with the available motor and a lack of proper attachment also hindered the experiments. Due to its design, the auger tended to strip inside the attachment device used to couple the auger with the motor. The auger's depth potential were unattainable because of this problem.

6.2.3. Custom Auger

The custom auger finally used for the study was manufactured based on research and a design by the University of Missouri Rolla. This auger was designed to propel the vehicle using a self digging mechanism. The custom auger was the only auger tested with the different sand compositions used in the study: Plain silica sand, a non-compacted sand mixture and a compacted sand mixture of sand, flour and oil. Like the conical auger first tested, the custom built auger was fabricated out of a high density polymer. However, during the plain sand experiments, this proved to be too big and heavy for the motor to drive through the medium. In the plain silica sand, the vehicle was able to bury three quarters of the auger before stalling out. Again, this stalling out is probably due to the large volume and surface area of the auger; the motor was simply not powerful enough to overcome the frictional forces encountered. In the non-compacted sand mixture experiments, the vehicle was able to fully bury the auger and three quarters of the motor. However, these results may not be a reflection of the true ability of the vehicle. Due to the low compaction of the mixture, the vehicle would sink in a few inches due to its own weight when simply placed on top of the medium. The mixture of the flour, sand and oil was very porous and thus gave the vehicle an extra advantage. This led to the experiments being repeated in the same sand mixture that had been highly compacted and was less porous. The results of the new runs showed that the vehicle was unable to dig as far as previous non-compacted experiments at low speeds, although it was able to reach previous depths when a full 15 V was supplied to the motor. With regard to the amount of torque needed to make the auger spin, the plain sand experiments were observed to require the highest torque followed by the compacted mixture and the

non-compacted mixture, falling in that order. The plain sand resulted in the highest friction due to the dry silica particles rubbing against the surface of the auger, while the addition of flour and oil helped reduce the friction between the medium and the auger surface.

6.3. Vehicle Experiments

6.3.1. Earthworm Concept

This experiment was run before the adapter shown in Figure 6 became available and therefore lacked a smooth transition surface between the auger and motor. The discontinuity, caused by the flat face of the motor, resulted in the sand becoming compacted at the point of transition from auger to motor, at which time the digging action ceased. It is likely that the resulting slippage of the attachment between the motor and the auger was the main reason for the subsequent lack of downward progress.

6.3.2. Air hose/friction reduction

A range of tube placements were tested: At the nose of the cone attachment, the beginning of the motor body and the middle of the motor body. At the nose of the cone attachment, there was no good way to fix the tubes in place that would allow them to remain stationary, so the tubes were forced to rotate with the cone if fixed to the surface. As a result, they flattened outward and curved upward as the vehicle penetrated into the sand, rendering them useless. When mounted in the middle of the motor body, the experiments generated unrepeatably results and in some runs even failed to penetrate far enough for the air to play an active role. In the experiments in which the vehicle did dig deep enough, the effect of the air hose was minimal. In the final location tested, at the beginning of the motor, it was observed that the air was focused into small areas at the

ends of the hoses and was not able to provide any assistance to the other areas of the sand to motor surface interface. In a further attempt to reduce the friction at the motor surface, small holes were drilled along the length of the air tubes. As the motor is of a radial design, the holes were not parallel with the surface, but at a tangent. A large number of design issues remained to be overcome in order for this system to be effective, so as with the experiments with fin design, this was deemed a secondary issue that could be returned to in future studies.

6.4. Biomimetic System

As mentioned in the previous chapter, various rodents were selected using the weighting system as warranting further examination for a study of the mechanisms they use to dig at shallow depths with arbitrary values. However, these rodents are not suitable as a model for this study because they dig with their claws and hind feet. They have no specifically adapted body parts, but are simply able to dig due to their small size and high strength. An investigation into replicating the movements and body of the mole may be more productive. The body of the mole consists of a tapered head, a streamlined body and highly adapted arms, all of which contribute to the mole's ability to dig quickly and powerfully.

The mole's arm and paw are highly adapted for digging. Its humerus bone is not like the long thin bones typically found in other mammals, but is as wide as it is long, making it almost rectangular in shape. To be able to handle moving large amounts of soil, the mole's back muscles (trapezius and latissimus dorsi) are directly connected to the humerus bone. In humans, these muscles indirectly affect the ability to move and lift with the arms. This muscle structure is unlike any other, and allows the paw to

extend out to the sides of the body and push directly back. The paw is already oriented outward with thick, long claws that easily penetrate soil. By pushing the soil outward, moles overcome the problems of sand movement. Other animals have to first loosen the soil, and then push it underneath their bodies and out of the tunnel. This is inefficient, as many strokes are needed. Moles can push their body into the material and then move the material behind them in one smooth stroke using a movement akin to swimming. After extending their arm and pushing the soil out to the sides, moles are then able to draw their paws close to the body and out in front of their face in tight spaces. This is only possible due to the unique design of the humerus bone.

The body is also of a desirable size as it is large enough so that scaling up results in no loss of the power to weight ratio, unlike in insects. One attribute that is highly useful is the mole's ability to turn 180 degrees inside relatively small tunnels. The tunnels moles construct are only a little more than the width of their body, although their body length is much longer. It is unknown how moles are able to contort their bodies to be able to accomplish this feat. The fur on the outside of the mole's body also helps in their movements. It is non-oriented, and this lack of a specific direction allows it to move in all directions freely, thus reducing the drag between the soil particles and the mole's body.

7. CONCLUSIONS

7.1. Shape Memory Alloys

The use of SMA to provide the mechanical power for a digging vehicle is a novel approach, but the design of the springs that are currently available leaves a lot to be desired. Large strokes can be obtained at low or no loads but were inefficient. At greater loads more energy input is necessary and considerably smaller strokes were achieved. Testing of each spring's power by recording the current and the subsequent time needed and distance traveled to lift a given amount of weight revealed that the efficiency is unsatisfactory for repeatable use and the stroke length decreased with every experiment. The fabrication of larger springs capable of lifting large loads increased the efficiency, but the "memory loss" effect became even more of an issue.

The first batch of springs, which were the smaller of the two sets, produced efficiencies (of electrical power to mechanical work transformation) as low as 0.003% with a maximum of 0.19%. The second batch of springs, which were larger, produced efficiencies between 0.23 – 0.56%. Although this is an improvement over the smaller springs, it is still well below the average energy conversion efficiency for a "typical" NiTi SMA, at 5%. One possible explanation for this low efficiency was that the heating cycled employed for the work was not optimized for the wires used. It is possible that the use of higher currents, for example 9-10 A, would decrease the amount of time needed for the wire to go through its transformation.

Further study is needed to determine the optimum balance between the two variables of current and applied force. Very little loss of the material's memory was observed in the first batch and the results were very repeatable. However the current and force applied for this phase were much lower, at a maximum of 6 A and 22 N, respectively, compared to those of the larger springs where testing started at 10 A and 45 N, respectively. The second batch showed signs of memory loss while testing was in progress and the effectiveness of the strokes decreased markedly with each successive run. These observations confirm those seen in previous experiments; although, the magnitude of the decline was not as extreme as those seen by previous recordings. Thus, it is possible that the lower currents were still deleterious but took longer to cause extreme damage. These two reasons make SMA springs an unpromising candidate to power a reusable digging vehicle.

7.2. Augers

7.2.1. Conical Augers

In measuring the amount of torque needed to drive the 127 & 140 mm conical augers through sand, they required the second highest values, exceeded only by the 203 mm diameter helical auger. During the colored sand experiment, it was observed that the sand was not displaced upward by the auger's action but outward. The thick flights, conical shape and overall design proved to be unreliable when used in a sand medium.

7.2.2. Helical Augers

The two similar diameter helical augers (63 mm, 76 mm) produced the smallest torque values, and succeeded in moving through the sand medium with less than 20 Nm to a depth of only 0.6 meters. The largest of the helical augers (203 mm diameter)

provided an excellent demonstration of how much the required torque increases as size increases, with over 160 Nm needed to penetrate half the depth (0.3 m) achieved by the two smaller augers. Unfortunately the amount of torque needed to move the large diameter helical auger exceeded what was possible using the motor that was available for the tests. The smaller diameter augers proved more suitable for this medium, although greater depths were not achievable as the vehicle's descent ceased due to a lack of weight on the bit or due to design issues such as the motor to auger attachment. Without additional weight, the vehicle experienced a type of buoyancy as the weight and power of the vehicle balanced the frictional forces needed to keep moving. If additional force was applied from above the vehicle would continue to dig, but once the force was removed the auger would again spin in place. A suitable attachment was also difficult to achieve with the helical augers. The thin center core made keeping the auger stationary with respect to the motor complicated, and as a result the augers tended to strip the inside of the attachment devices used to couple the auger with the motor. The design of the helical augers was therefore deemed unsuitable for a self propelled digging vehicle.

7.2.3. Custom Auger

The custom auger tested in this study was designed specifically for digging in sand and was tested using three different sand media: plain silica sand and a mixture of sand, flour and oil that was either compacted or un-compacted. All the tests used fixed voltages of 5, 10 and 15 V. The plain sand trials proved to require the most power as the estimated digging energy was higher than that for the other two trials for all three of the fixed voltages tested. The non-compacted sand mixture did not constitute a realistic experiment as the porous medium allowed the vehicle to start to sink, thus artificially

increasing the depth achieved, due to its weight alone, before digging even started. The torque in the plain sand experiments rivaled that of the conical auger at 135 Nm, but was significantly less in both the sand mixtures. The custom auger thus presented a viable alternative to the other augers tested, but as the focus of the project changed, the auger tests did not proceed further.

7.3. Biomimetic System

The time frame of the project allowed a detailed and descriptive review of a range of biological organisms to be conducted. In order to maximize the data gathered without focusing on the lack of data for any one organism, a small database of fossorial creatures was established. Using the available knowledge for each organism, a weighted system was created that allowed the output of different animals for different scenarios to be compared.

Even though the mole did not out perform the other animals for all the theoretical environments considered, its muscular and frame structure deserve a closer look as part of an attempt to construct a new model for a digging vehicle. The weighting system used in this comparison was based on speed, depth, power, material substance, mechanical complexity, geographic range and the size of the body of the creature, and confirmed that the mole was the best candidate out of the 43 examined for depths of less than 6 m (240 in) and a body length of less than .3 m (12 in). The mole's body size, geographic range and digging depth are well suited to vehicle modeling. The mole has many attributes that can be viewed as highly desirable, such as its unique digging movement, the large aspect ratio of its digging apparatus, and its cylindrical and streamlined body structure.

The researcher therefore recommends that future research should focus on the Townsend mole, rather than any of the other organisms surveyed. The results for the mole can be found in Appendix K.

8. FUTURE RESEARCH

Many of the augers tested in this study were not designed specifically for self propulsion through a sand media. The UM-Rolla (UMR) auger, however, is designed to do so and has the potential to dig to great depths. Although the UMR auger discussed in this thesis was much too large for the available motor to handle, a scaled down version might accomplish the research objective, namely constant and steady penetration. By scaling down the size of the auger, the motor will need less power to turn it and therefore will have more in reserve to compensate for the increasing frictional forces at greater depths. The vehicle's digging ability could also be enhanced through the addition of a vibration mechanism. The use of a fluid media might also prove beneficial. The use of air to boost the auger's digging action in this study was a quick and rough experiment that returned only an inconclusive result. This approach may merit a more detailed and better researched trial. The use of vibration and/or fluid media in various other digging devices are known to assist in the digging process by removing the digging media, such as the use of water based fluids in oil drilling platforms.

The next step in the effort to advance the research into biomimetic devices is to determine the exact mechanism by which a mole's swimming motion propels it through the earth and measure the forces involved. This would enable detailed models to be constructed using various body sizes and speeds.

This thesis has provided only the very beginning stages of researching new and innovative approaches to mechanical digging; much more research, design and testing is needed to accomplish a comprehensive theoretical treatment and working demonstration model.

REFERENCES

1. Maciejewski, J. and Jarzebowski, A.; "Laboratory optimization of the soil digging process," *Journal of Terramechanics*, vol. 39, 2002, pp. 161-179.
2. Sellmann, P.V. and Brockett, B.E.; "Bit Design Improves Augers," *The Military Engineer*, Vol. 79, August, 1987, pp. 453-454.
3. Chugh, C.P.; Manual of Drilling Technology, A.A. Balkema/Rotterdam, India. 1985, pp. 1-45.
4. Onshore Drilling, http://www.naturalgas.org/naturalgas/extraction_onshore.asp, 2005
5. Petroleum Extraction, <http://www.personal.psu.edu/users/c/b/cbm134/history.htm>, 2005
6. Institute for Energy Research, http://instituteforenergyresearch.org/Energy_Timeline.htm, 2005
7. Maciejewski, J., Jarzebowski, A. and Trampczynski, W.; "Study on the efficiency of the digging process using the model of excavator bucket," *Journal of Terramechanics*, vol. 40, 2004, pp.221-233.
8. Abo-Elnor, M., Hamilton, R. and Boyle, J.T.; "Simulation of soil-blade interaction for sandy soil using advanced 3D finite element analysis," *Soil & Tillage Research*, vol. 75, 2004, pp. 61-73.
9. Georgiadis, K., Potts, D.M. and Zdravkovic, L.; "Modelling the shear strength of soils in the general stress space," *Computers and Geotechnics*, vol. 31, 2004, pp. 357-364.
10. Finite Element Analysis Modeling Issues and Ideas, http://www3.sympatico.ca/peter_budgell/Modeling_issues.html#C1, 2005
11. Anonymous; "Trenchless technology speeds gas line renewals", *Pipeline & Gas Journal*, vol. 222, 1995, pp.23-25.

12. Stidger, Ruth. W.; "Technology: Trenchless technology provides environmental advantages", *Gas Utility Manager*, vol. 47, November, 2002. p.18-19.
13. Friant, J.E. and Oxdemir, L.; "Tunnel Boring Technology – Present and Future", *Proceedings of the Rapid Excavation and Tunneling Conference*, 1993, pp.869-888.
14. Worthington, T.; "New Tools for Tunneling, Finding Niches in Hardrock", *Engineering and Mining Journal*, vol. 204, February, 2003, pp.32-34.
15. Normile, D.; "Cutting Corners," *Popular Science*, vol. 246, April, 1995, pp 27.
16. Hill, J.L. III, Shenhar, J. and Lombardo, M.; "Tethered, Down-Hole-Motor Drilling system – A benefit to Mars exploration," *Advanced Space Research*, vol. 31, 2003, pp.2421-2426
17. Krajick, K.; "New drills augur a great leap downward" *Science*, vol. 283, 1999, pp.781.
18. Mavroidis, C.; Pfeiffer, C. and Mosley, M.; "Conventional actuators, shape memory alloys and electrorheological fluids", *Research in Nondestructive Testing*, vol. 14, 2002, pp.1-32.
19. Shape Memory Alloys,
http://www.cs.ualberta.ca/~database/MEMS/sma_mems/sma.html, 2005
20. Gale, W.F.; Auburn University Materials Research and Education Center, personal communication.
21. Introduction to Shape Change and Superelasticity,
<http://www.jmmedical.com/html/introduction.html>, 2005.
22. Huang, W.; "On the selection of shape memory alloys for actuators", *Materials and Design* 23, 2002, pp.11-19.
23. Park, B., Shantz, M. and Prinz, F.; "Scalable rotary actuators with embedded shape memory alloys", *Proc. Of The International Society for Optical Engineering*, vol. 4327, 2001, pp.79-87.
24. Paulson, L.; "Biomimetic robots", *Computer Magazine*, September 2004, pp.48-53.
25. <http://www.first-to-fly.com/History/History%20of%20Airplane/history.htm>, 2005

26. <http://inventors.about.com/library/weekly/aa091297.htm>, 2005
27. Vanderbuilt, T.; “Evolution of the gearhead”, DigitAll Magazine, summer 2004, http://www.samsung.com/DigitAll/BrandCampaign/magazinedigitall/2004_summer/feat_04a.htm
28. Isla, D.; “RoboTuna project to model real fish”, The Tech Magazine, Vol. 115, Number 49, 1995, pp. 13, 23.
<http://www-tech.mit.edu/Issue/V115/N49/robotuna.49n.html>
29. Sheenan, C.; “Robotics gains in prestige, in part due to military conflicts” Associated Press April 2004.
<http://www.aaai.org/AITopics/html/archvE4.html#april8b>
30. Brain, M.; Personal BLOG: Robotic Nation Evidence, article “Formerly arcane research gets new respect” April 2004
<http://roboticnation.blogspot.com/2004/04/future-of-robotic-police.html>
31. Weed, W.; “This is your computer speaking...” Discover Magazine, Volume 23 No. 8 August 2002.
<http://www.aaai.org/AITopics/html/autveh.html>
32. News office; “MITs robotic helicopter makes first aerobatic roll” February 2002
<http://web.mit.edu/newsoffice/2002/robochopper.html>
33. DARPA Grand Challenge 05
<http://www.darpa.mil/grandchallenge/overview.html>
34. <http://www.vattenkikaren.gu.se/fakta/arter/mollusca/bivalvia/ensiamer/ensiam2e.html>, 2005
35. <http://www.ecy.wa.gov/programs/sea/pugetsound/species/geoduck.html>, 2005
36. http://www.liveaquaria.com/product/prod_Display.cfm?siteid=23&pCatId=579, 2005
37. <http://www.chesapeakebay.net/shipworm.htm>, 2005
38. <http://molecrickets.ifas.ufl.edu/mcri000b.htm>, 2005
39. <http://molecrickets.ifas.ufl.edu/mcri0001.htm>, 2005
40. <http://www.dpi.qld.gov.au/beef/13129.html>, 2005
41. <http://www.ces.ncsu.edu/depts/ent/clinic/Bugofwk/970081/dungbeet.htm>, 2005

42. <http://ianrpubs.unl.edu/Insects/g1062.htm>, 2005
43. <http://www.scienceinafrica.co.za/2004/april/trapdoor.htm>, 2005
44. <http://www.zo.utexas.edu/research/txherps/frogs/rhinophrynus.dorsalis.html>, 2005
45. <http://animaldiversity.ummz.umich.edu/site/accounts/information/Rhinophrynidae.html>, 2005
46. http://animaldiversity.ummz.umich.edu/site/accounts/information/Perognathus_flavescens.html, 2005
47. http://animaldiversity.ummz.umich.edu/site/accounts/information/Perognathus_fasciatus.html, 2005
48. http://animaldiversity.ummz.umich.edu/site/accounts/information/Thomomys_talpoides.html, 2005
49. <http://animaldiversity.ummz.umich.edu/site/accounts/information/Geomyidae.html>, 2005
50. http://animaldiversity.ummz.umich.edu/site/accounts/information/Heterocephalus_glaber.html, 2005
51. http://animaldiversity.ummz.umich.edu/site/accounts/information/Scapanus_townsendii.html, 2005
52. <http://sandia.gov/media/NewsRel/NR2001/minirobot.htm>, 2005
53. Mondada, F. and Guignard, A.; “SWARM-BOT: From Concept to Implementation”, Proceeding of the 2003 IEEE/RSJ. Intl. Conference on Intelligent Robots and Systems, Las Vegas, Nevada, October 2003.
54. Kahn, J.M., Katz, R.H. and Pister, K.S.J.; “Next Century Challenges: Mobile Networking for “Smart Dust””, Proceeding of the 1999 5th Annual ACM/IEEE International Conference on Mobile Computing and Networking (MobiCom’99), 1999, p.271-278.
55. Stormont, D.P.; “Robot swarms for planetary exploration”, Proc. 4th International Conf. and Exposition/Demonstration on Robotics for Challenging Situation and Environments, 2000, p.347-352.

56. Fukuda, T., Mizoguchi, H., Sekiyama, K. and Arai, F.; “Group behavior control for MARS (Micro Autonomous Robotic System)”, Proc. 1999 IEEE International Conf. on Robotics and Automation, May 1999. pp.1550-1555.
57. Kdrovach, B.A., and Lamont, G.B.; “A particle swarm model for swarm-based networked sensor systems”, Proc. Of the ACM Symposium on Applied Computing, 2002 p.918-924.
58. Kube, C.R. and Bonabeau, E.; “Cooperative transport by ants and robots”, Robotics and Autonomous Systems, vol. 30, 2000, p.85-101
59. Fukuda, T., Funato, D., Sekiyama, K. and Arai, F.; “Evaluation on flexibility of swarm intelligent system”, Proc. 1998 IEEE International Conf. on Robotics and Automation, May 1998, p.3210-3215.
60. Dudek, G., Jenkin, M.; “A taxonomy for swarm robots”, Proc. 1993 IEEE/RSJ International Conf. on Intelligent Robots and Systems, July 1993, p.441-447.
61. <http://www.sandia.gov/media/NewsRel/NR2000/avalanch.htm>.
62. Russell, R.A.; “Pheromone communication: Implementation of necrophoric bee behavior in a robot swarm”, Proc. 2004 IEEE Conf. on Robotics, Automation and Mechatronics, December 2004, p.638-643.
63. Lam, Y.K., Wong, E.K. and Loo, C.K.; “Explicit communication in designing efficient cooperative mobile robotic system”, Proc. 2003 IEEE International Conf. on Robotics and Automation, September, 2003. p.3869-3874.
64. Owusu, Yaw A.; “Physical-chemical study of sodium silicate as a foundry sand binder”, Advances in Colloidal Interface Science, September, 1982. p.57-91.
65. Cash, Alex ; Air Force Research Lab, Eglin Air Force Base, Fl., personal communication.

APPENDICES

Appendix A. Draft CAD Drawing of Conical Auger

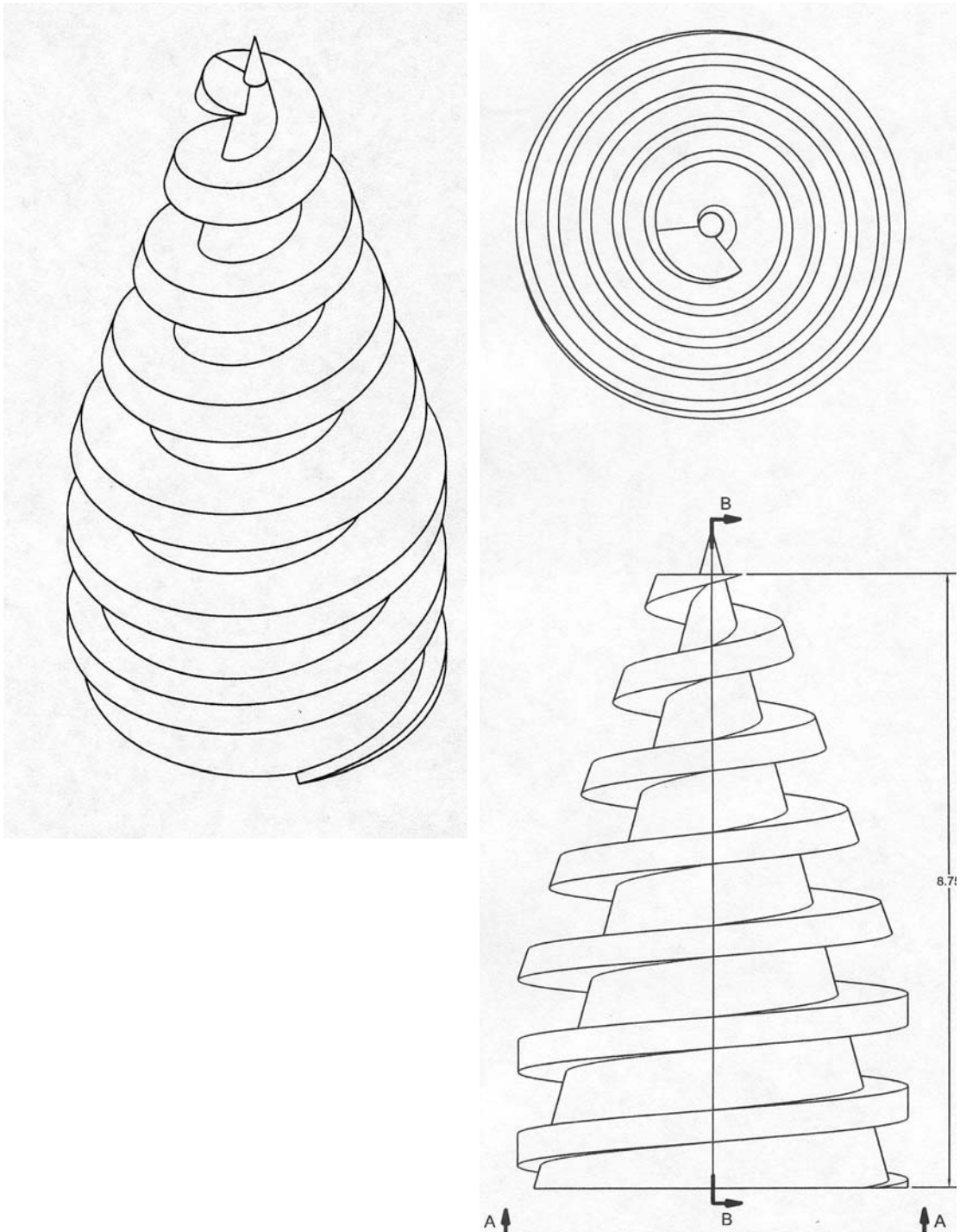


Figure A-1: View of Conical Auger

Appendix A. Draft CAD Drawing of Conical Auger

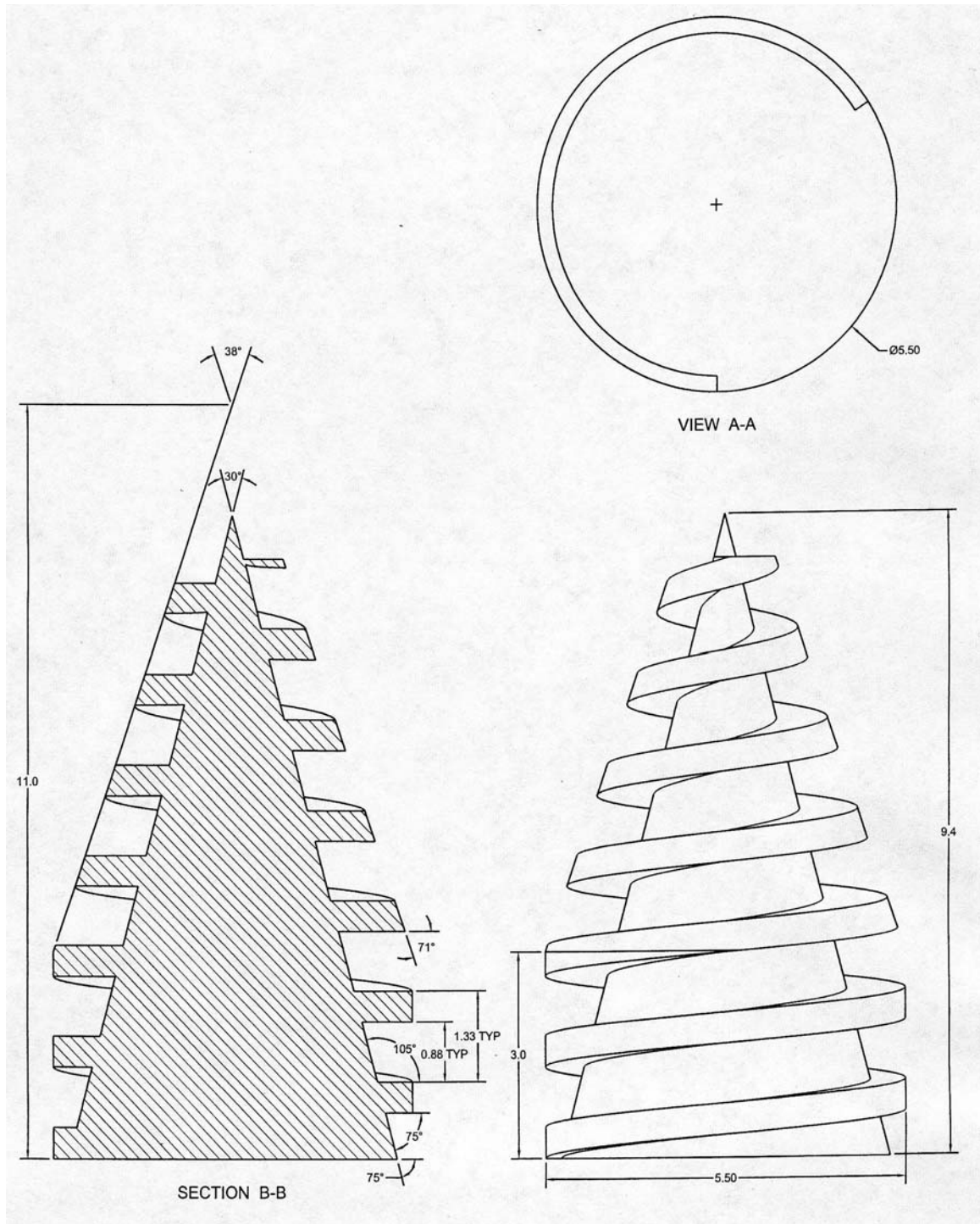


Figure A-2: View of Conical Auger

Appendix B. Auger and Motor with Fin Design



Figure B-1: Motor with three small fins



Figure B-2: Motor and conical auger with two large fins

Appendix B. Auger and Motor with Fin Design



Figure B-3: Motor and conical auger with rod-fin design

Appendix C. Extended Auger



Figure C-1. Extended auger used for pull test

Appendix E. List of Initial Questions

List of questions pertaining to insects/mammals/fish/amphibians that “dig”

- Does the organism carry the material displaced away?
- Does the organism gain sustenance from the material?
- If the organism digs mechanically, then:
 - Does the organism push or scrape at the dirt?
 - If scrape, then:
 - Brief description of digging apparatus (*e.g.* claws)
 - Any interesting characteristics of the digging apparatus?
 - Aspect ratio of the digging apparatus?
 - Does the same apparatus serve other functions?
 - Defense
 - Utility
 - If push, then:
 - Does the organism push the material to the side?
 - Does the organism push the material behind its body?
 - Other movements?
 - Which limbs does the organism use?
 - Front, back or both?
 - Does the organism use any other body parts to assist with digging?
 - How far does the organism dig?
 - Just enough to cover itself?
 - Further?
 - If so, estimated depth by body length. (*e.g.* 2 times its length)
 - Estimated speed (absolute or relative to body length)?
 - Why does the organism dig?
 - Protection
 - Food
 - Hibernation
 - Housing/shelter
 - Other
 - Does the organism need/use help from symbiotic organisms?
 - If so, how do they help each other?
 - How closely related are the species involved?
- How big are its limbs compared to its body?
 - Describe how the limbs move
 - Swimming motion
 - Overhand motion
 - Multi-jointed

Appendix E. List of Initial Questions

- How much weight can the organism carry/push/move compared to its own body weight?
 - Example: an ant can carry ~10X its body weight
- Estimated size of organism (dimensions)

Questions pertaining to basic organism information

- What unique capability/function helps the insect survive?
- What type of environment does the organism live in?
 - Can the organism survive in a low nutrient (*e.g.* almost pure water) environment?
 - Nocturnal?
- Average life span?
- Major sensing mechanism?
 - Eyes
 - Antennae
 - Vibration
 - Other
- How does the organism communicate?
 - Chemical
 - Vocal
 - Movement/gesture
- Defense Mechanisms?
 - Stealth/protective coloring
 - Odor
 - Chemical Secretion
 - Claws *etc.*
 - None
 - Other
- Eating habits?
 - Carnivore
 - Herbivore
 - Omnivore
 - Other (*e.g.* gains energy from soil or converts sunlight as in photosynthesis)

Appendix F. Scenarios for Weighted Values

Table F-1: Weighted values for three scenarios

Weightings	Scenario 1 (shallow depths, small body size)	Scenario 2 (medium depths, small body size)	Scenario 3 (deep depths, medium body size)
Size of body	30%	25%	15%
Speed	25%	15%	10%
Mechanical Complexity	15%	15%	10%
Hard Substances	10%	10%	10%
Geographic Range	10%	10%	5%
Power	5%	10%	30%
Depth	5%	15%	20%
Totals	100%	100%	100%

- Weighted = Arbitrary values included
- Weighted = Only known values
- Data Input
- Maximum value output for scenario

Scenario 1

Size of Body (<30cm; 12in)
 Depth (<152cm; 60in)

Scenario 2

Size of Body (<30cm; 12in)
 Depth (152cm;60in<X<610cm;240in)

Scenario 3

Size of Body
 (30cm;12in<X<91cm;36in)
 Depth (>610cm;240in)

Appendix G. Biometric Flowchart

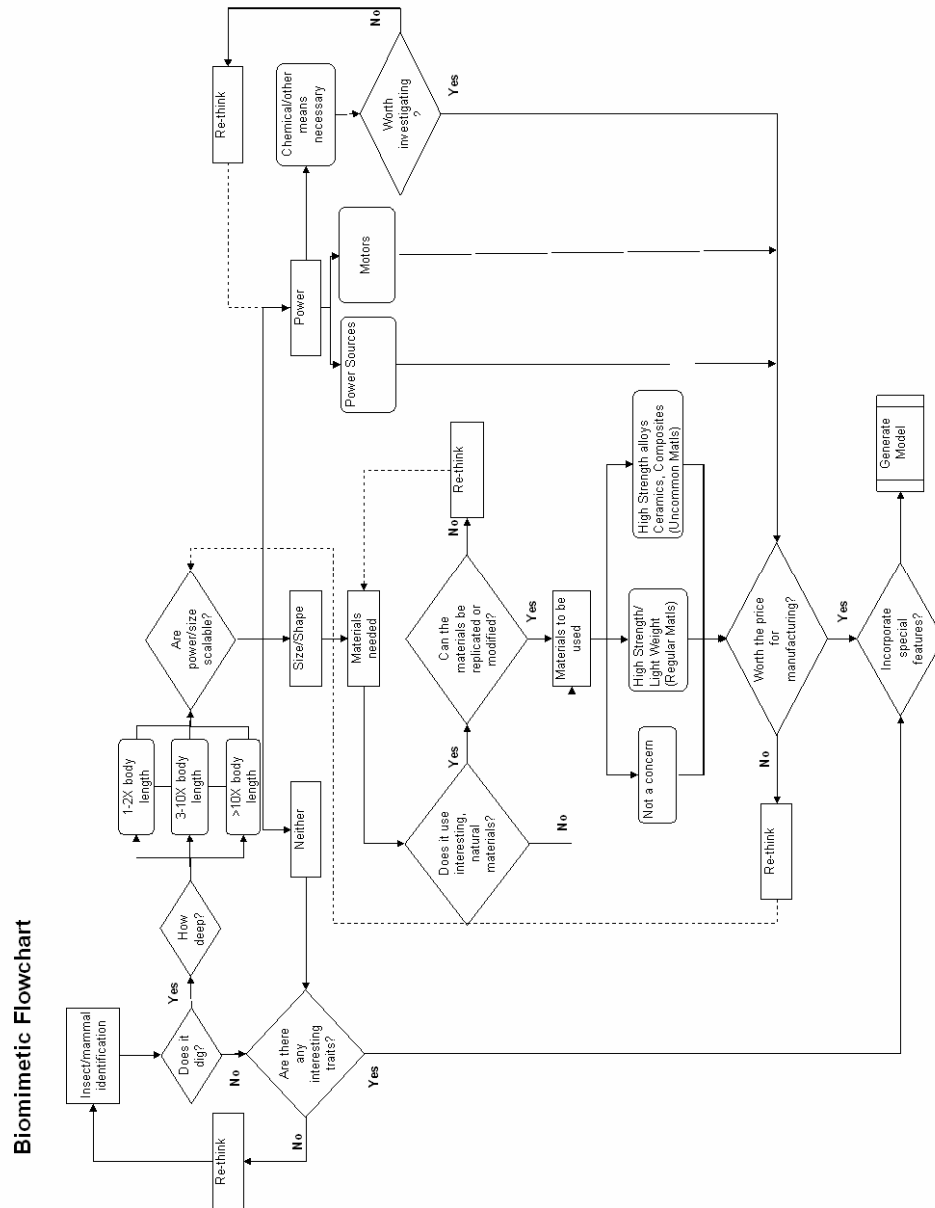


Figure G-1: Biomimetic Flowchart

Appendix H. SMA Spring Data

Table H-1. Results of Spring 1 with 44.5 N at various currents.

44.5N (10 lbs)		
Observation	Time (s)	Distance (mm)
20 A		
1	12	170
2	15	165
3	15	160
18 A		
1	14	155
2	12	150
3	12	150
16 A		
1	12	150
2	14	140
3	14	140
14 A		
1	17	135
2	16	135
3	15	130
12 A		
1	23	130
2	21	125
3	24	130
10 A		
1	36	125
2	35	125
3	35	125

Appendix H. SMA Spring Data

Table H-2. Results of Spring 2 showing the differences in actuation distance (mm) with a load of 44.5 N at various currents

44.5N (10 lbs)		
Observation	Initial Test	2nd Testing
10 A		
1	150	105
2	140	105
3	140	105
12 A		
1	140	110
2	140	110
3	135	110
14 A		
1	140	115
2	140	115
3	140	115
16 A		
1	135	115
2	135	115
3	135	115

Table H-3. Results of Spring 3 showing the differences in actuation distance (mm) at low currents with a load of 26.7 N

26.7N (6 lbs)		
Observation	Initial Test	2nd Testing
9A		
1	195	170
2	190	170
3	185	170
8A		
1	175	165
2	175	165
3	170	165
7A		
1	170	160
2	165	160
3	165	155

Appendix I. Final Results for all Creatures

Table I-1. Final Results for all Creatures

Specimens	Scenario 1:	Scenario 1:	Scenario 2:	Scenario 2:	Scenario 3:	Scenario 3:
Razor Clam	6.9	3.3	6.9	4.2	7.9	3.7
Geoduck Clam	6.5	3.65	5.95	3.7	6.65	2.75
Common Piddock	7.95	4.05	7.7	4.1	9.3	3.9
Peanut Worm	6.45	2.55	6.05	2.45	7.3	1.9
Ship Worm	7.05	3.45	6.75	3.45	8.5	3.1
June Bug/Grub	6.65	3.05	5.85	3.15	6.7	2.5
Dung Beetle	8	4.25	6.8	3.95	7.5	3.3
Mole Cricket	7.05	3.45	6.75	4.05	7.7	3.5
Termite	8.5	5.2	7.9	5.5	9.9	5.7
Cicadas	6.75	3.15	6	3.3	6.9	2.7
Trapdoor Spider	6.75	3.6	6	3.75	7.2	3
Carpenter Bee	6.45	3.9	5.95	4	7.55	3.65
Blind Snakes	6.85	3.25	6.3	3.6	7.1	2.9
Mexican Burrowing Toad	6.85	2.2	6.45	2.1	7.3	1.6
Tiger Salamander	7.95	4.2	7	4.15	7.35	2.85
Plains Pocket Mouse	7.75	4	6.65	4.1	7.45	2.95
Olive Backed Pocket Mouse	7.95	4.2	7.25	4.7	8.05	3.55
Brown Rat	8.55	4.5	7.75	4.3	8.55	2.85
Narrow-Faced Kangaroo Rat	8.55	4.5	7.75	4.3	8.55	2.85
Gulf Coast Kangaroo Rat	7.75	4.45	7.2	4.2	8.2	2.8
Malagasy Giant Rat	8.45	4.7	7.9	5.35	8.55	4.05
Yellow Cheeked Vole	7.3	4.3	6.35	4.25	7.25	3.05
Long Tailed Vole	7.95	3.9	7.25	3.8	8.25	2.55
Conovers Tuco Tuco	7.6	4.6	6.6	4.5	7.55	3.35
Golden Mantled Ground Squirrel	8.55	4.8	7.6	5.05	8.15	3.65
Washington Ground Squirrel	7.75	4.45	7.2	4.2	8.2	2.8
Idaho Ground Squirrel	7.7	4.7	6.9	4.8	7.6	3.4
Northern Pocket Gopher	7.75	4.45	7.2	4.8	7.45	3.25
Western Pocket Gopher	7.75	3.7	6.65	3.8	7.25	2.75
Valley Pocket Gopher	8.25	4.2	7.65	4.8	8	3.5
Camas Pocket Gopher	8.05	4.45	7.45	4.15	8.15	2.75
Black Capped Marmot	7.65	2.7	7.2	2.55	8.45	2.45
Fat Tailed Gerbil	6.8	3.65	6.15	3.9	7.2	3
Great Gerbil	8.35	4.75	8	5.3	8.75	4.55
Indian Gerbil	7.3	4.15	6.35	4.1	7.15	2.95
Townsend Mole	7.95	5.7	7.5	5.85	7.95	4.05
Hairy Tailed Mole	7.6	5.35	6.65	5	7.35	3.45
Pink Fairy Armadillo	7.45	4.15	6.95	3.95	8.05	2.65
Giant Armadillo	7.15	3.85	6.7	3.7	8.5	3.1
African Striped Weasel	8.05	4.75	7.45	4.45	8.2	2.8
Stink Badger	7.75	4.45	7.2	4.2	8.35	2.95
Naked Mole Rats	8.25	5.1	7.6	5.35	8.2	4
African Mole Rat	8.45	5	7.55	4.4	8.2	2.8

Appendix J. Information Found for Each Creature

Creature	Specific Information Found				
	Digging depths (cm)	Depth to body length ratio	Body Length (cm)	Digging Material	Speed
Razor Clam	150-600	20-40	8-15	loose soil	
Geoduck Clam	91	5	19	water, mud	30 cm/yr
Common Piddock			12	rock	
Peanut Worm			1-7	water, loose soil	
Ship Worm			60	wood	
June Bug/Grub	10	8	1	top soil	
Dung Beetle	30	6	1-5	compact soil	
Mole Cricket	152	30	4-5	loose soil, sand	
Termite	4570	>25	<1	wood, soil	
Cicadas	30-60	12	2-5	compact soil	
Trapdoor Spider	30	12	2-5	loose soil	
Carpenter Bee	8	20	2-5	wood	2 cm/6 days
Blind Snakes	200	10	15-20	loose soil	
Mexican Burrowing Toad			5-7	loose soil	
Tiger Salamander	60	2	17-33	loose soil	
Plains Pocket Mouse	15-20	5	14	loose soil	
Olive Backed Pocket Mouse	200	14	12-14	loose soil	
Brown Rat			32	loose soil	
Narrow-Faced Kangaroo Rat			32	loose soil	
Gulf Coast Kangaroo Rat			20-27	loose soil	
Malagasy Giant Rat	500	14	30-35	loose soil	
Yellow Cheeked Vole	30	2	14-18	loose soil	
Long Tailed Vole			10-18	loose soil	
Conovers Tuco Tuco	30	1	33-44	loose soil	
Golden Mantled Ground Squirrel	100-200	6	30	loose soil	
Washington Ground Squirrel			19-25	loose soil	
Idaho Ground Squirrel	50-121	5	21-26	loose soil	
Northern Pocket Gopher	200	10	21	loose soil	
Western Pocket Gopher	10-15	1	15	loose soil	

Appendix J. Information Found for Each Creature

	Digging depths (cm)	Depth to body length ratio	Body Length (cm)	Digging Material	Speed
Valley Pocket Gopher	100-300	10	11-33	loose soil	
Camas Pocket Gopher			33	loose soil	
Black Capped Marmot			53-73	compact soil	
Fat Tailed Gerbil	100	9	11	loose soil	
Great Gerbil	150-250	15	15-20	clay, compact soil	
Indian Gerbil	50	3	15-17	loose soil	
Townsend Mole	300	14	21	loose soil	5.5 m/hr
Hairy Tailed Mole	45-70	5	12-14	loose soil	4.5 m/hr
Pink Fairy Armadillo			13-15	loose soil	
Giant Armadillo			90	compact soil	
African Striped Weasel			25-35	loose soil	
Stink Badger			39	loose soil	
Naked Mole Rats	200	20	10	loose soil	
African Mole Rat			11-17	loose soil	

Appendix K. Metric Results for the Townsend Mole

Table K-1. Metric Results for the Townsend Mole

Speed

<u>Length to width ratio of digging apparatus</u>		Value	Known Values
Ratios			
0.9-1.9		5	
0.89-0.8	2.0-2.9	4	
0.79-0.7	3.0-3.9	3	
0.69-0.6	4.0-4.9	2	
0.59-0.5	5.0-5.9	1	
<0.5	>6	0	
Given Value:		3	0
<u>Size of digging apparatus to size of body ratio</u>		Value	Known Values
Ratios			
25-30%		5	
20-24%	30-34%	4	
15-19%	35-39%	3	
10-14%	40-44%	2	
5-9%	45-49%	1	
<5%	>50%	0	
Given Value:		3	0
<u>Number of strokes per unit time</u>		Value	Known Values
Strokes per minute			
>25		5	
20-25		4	
15-20		3	
10-15		2	
1-10		1	
Given Value:		3	0
<u>Coordinated vs random team effort</u>		Value	Known Values
Type			
Coordinated effort		5	
Unknown		3	
Random effort		1	solitary
Given Value:		1	1
<u>Raw Speed</u>		Value	Known Values
Rate			
Very Fast		5	
Slightly Fast		4	5.5m/hr
Intermediate		3	
Slightly Slow		2	
Very Slow		1	
Given Value:		4	4

Appendix K. Metric Results for the Townsend Mole

Distance moved in one stroke

Amount	Value	Known Values
>50% body length	5	
35-49% body length	4	
20-34% body length	3	
5-19% body length	2	
1-4% body length	1	
Given Value:	3	0
	17	5

Depth

Applied force

Force	Value	Known Values
>85% of its body weight	5	
70-84% of its body weight	4	
55-69% of its body weight	3	
40-54% of its body weight	2	
25-39% of its body weight	1	
<24% of its body weight	0	
Given Value:	3	0

Depth to body length ratio

Overall ratio	Value	Known Values
>25X body length	5	
20-25X body length	4	
15-20X body length	3	
10-15X body length	2	14x
1-10X body length	1	
Given Value:	2	2

Appendix K. Metric Results for the Townsend Mole

Appropriate depth	Scenario 1		Scenario 2		Scenario 3	
	Value	Known Values	Value	Known Values	Value	Known Values
Appropriate level						
Highly appropriate	5		5	300cm; 118in	5	
Slightly appropriate	4		4		4	
Indifferent	3	300cm; 118in	3		3	300cm; 118in
Slightly inappropriate	2		2		2	
Very Inappropriate	1		1		1	
Given Value:	3	3	5	5	3	3
	8	5	10	7	8	5

Power

Size of digging apparatus to size of body ratio

Ratios	Value	Known Values
25-30%	5	
20-24%	4	
15-19%	3	
10-14%	2	
5-9%	1	
<5%	0	
Given Value:	3	0

Applied Force

Force	Value	Known Values
>85% of its body weight	5	
70-84% of its body weight	4	
55-69% of its body weight	3	
40-54% of its body weight	2	
25-39% of its body weight	1	
<24% of its body weight	0	
Given Value:	3	0

Appendix K. Metric Results for the Townsend Mole

<u>Material Hardness</u>		Value	Known Values
Type			
Rock		5	
Clay		4	
Wood		3	
Compact Soil		2	
Loose Soil		1	
Sand		1	
	Given Value:	1	1
		7	1

Hard Substances

<u>Chemical Capabilities</u>		Value	Known Values
Capability			
Yes		5	
Unknown		3	
No		1	
	Given Value:	1	1

<u>Applied Force</u>		Value	Known Values
Force			
>85% of its body weight		5	
70-84% of its body weight		4	
55-69% of its body weight		3	
40-54% of its body weight		2	
25-39% of its body weight		1	
<24% of its body weight		0	
	Given Value:	3	0

<u>Material Hardness</u>		Value	Known Values
Type			
Rock		5	
Clay		4	
Wood		3	
Compact Soil		2	
Loose Soil		1	
Sand		1	
	Given Value:	1	1
		5	2

Appendix K. Metric Results for the Townsend Mole

Mechanical Complexity*

		<u>Motion complexity while digging</u>	Value	Known Values
Complexity level			1	
Five or more movements			2	
Four movements			3	
Three movements			4	
Two movements			5	
Single movement			5	
List of movements:	Swim motion			
	Given Value:		5	5
	<u>Material Processing</u>			
Type			Value	Known Values
Compaction			1	
Unknown			3	
Removal			5	
	Given Value:		5	5
	<u>Chemical Capabilities</u>			
Capability			Value	Known Values
Yes			1	
Unknown			3	
No			5	
	Given Value:		5	5
			15	15

* Values are inverted: A high mechanical complexity is unfavorable

Geographic Range		Value	Known Values
Appropriate Level			
Highly appropriate		5	
Slightly appropriate		4	
Indifferent		3	
Slightly inappropriate		2	
Very Inappropriate		1	
	Given Value:	5	5
		5	5

Appendix K. Metric Results for the Townsend Mole

Size of body	Scenario 1		Scenario 2		Scenario 3	
Appropriate Level	Value	Known Values	Value	Known Values	Value	Known Values
Highly appropriate	5		5		5	
Slightly appropriate	4	21cm;8in	4	21cm;8in	4	
Indifferent	3		3		3	
Slightly inappropriate	2		2		2	21cm;8in
Very Inappropriate	1		1		1	
Given Value:	4	4	4	4	2	2
	4	4	4	4	2	2

Total Value

	Scenario 1	Scenario 2	Scenario 3			
Speed	4.25	1.25	2.55	0.75	1.7	0.5
Depth	0.4	0.25	1.5	1.05	1.6	1
Power	0.35	0.05	0.7	0.1	2.1	0.3
Hard Substances	0.5	0.2	0.5	0.2	0.5	0.2
Mechanical Complexity	0.75	2.25	0.75	2.25	1.5	1.5
Size of Body	1.2	1.2	1	1	0.3	0.3
Geographic Range	0.5	0.5	0.5	0.5	0.25	0.25
Total Value	7.95	5.7	7.5	5.85	7.95	4.05

Raw score with arbitrary values
Raw Score without arbitrary values
Weighted = Arbitrary values included
Weighted = Only known values
Information Unknown = Arbitrary value of 3
Information Known
Data Input